EuroIntervention 2019;14:e1568-e1577 published online November 2018 ■ published online e-edition February 2019

Joint consensus on the use of OCT in coronary bifurcation lesions by the European and Japanese bifurcation clubs

Yoshinobu Onuma[1], MD, PhD; Yuki Katagiri[2], MD; Francesco Burzotta[3], MD; Niels Ramsing Holm[4], MD; Nicolas Amabile[5], MD, PhD; Takayuki Okamura[6], MD, PhD; Gary S. Mintz[7], MD; Olivier Darremont[8], MD; Jens Flensted Lassen[9], MD, PhD; Thierry Lefèvre[10], MD; Yves Louvard[10], MD; Goran Stankovic[11], MD, PhD; Patrick W. Serruys[12]*, MD, PhD

1. Thoraxcenter, Erasmus Medical Center, Rotterdam, the Netherlands; 2. Academic Medical Centre, University of Amsterdam, Amsterdam, the Netherlands; 3. Institute of Cardiology, Catholic University of the Sacred Heart, Rome, Italy; 4. Department of Cardiology, Aarhus University Hospital, Skejby, Aarhus, Denmark; 5. Cardiology Department, Institut Mutualiste Montsouris, Paris, France; 6. Department of Medicine and Clinical Science, Yamaguchi University Graduate School of Medicine, Ube, Japan; 7. Cardiovascular Research Foundation, New York, NY, USA; 8. Clinique St. Augustin, Bordeaux, France; 9. Department of Cardiology, The Heart Centre, Rigshospitalet, University of Copenhagen, Copenhagen, Denmark; 10. Ramsay Générale de Santé - Institut Cardiovasculaire Paris Sud, Hopital Privé Jacques Cartier, Massy, France; 11. Department of Cardiology, Clinical Center of Serbia, and Medical Faculty, University of Belgrade, Belgrade, Serbia; 12. International Centre for Circulatory Health, NHLI, Imperial College London, London, United Kingdom

GUEST EDITOR: Adnan Kastrati, MD; *Deutsches Herzzentrum München, Munich, Germany*

This paper also includes supplementary data published online at: http://www.pcronline.com/eurointervention/148th_issue/269

KEYWORDS

- bifurcation
- bioresorbable scaffolds
- drug-eluting stent
- optical coherence tomography

Abstract

Coronary artery bifurcation lesions comprise approximately 15-20% of all percutaneous coronary interventions (PCI) and constitute a complex lesion subgroup. Intravascular optical coherence tomography (OCT) is a promising adjunctive tool for guiding coronary bifurcation with its unrivalled high resolution. Compared to angiography, intravascular OCT has a clear advantage in that it depicts ostial lesion(s) in bifurcation without the misleading two-dimensional appearance of conventional angiography such as overlap and foreshortening. In addition, OCT has the ability to reconstruct a bifurcation in three dimensions and to assess the side branch ostium from 3D reconstruction of the main vessel pullback, which can be applied to ensure the optimal recrossing position of the wire after main vessel stenting. Recently, online co-registration of OCT and angiography became widely available, helping the operator to position a stent in precise landing zones, reducing the risk of geographic miss. Despite these technological advances, the currently available clinical data are based mainly on observational studies with a small number of patients; there is little evidence from randomised trials. The joint working group of the European Bifurcation Club and the Japanese Bifurcation Club reviewed all the available literature regarding OCT use in bifurcation lesions and here provides recommendations on OCT guiding of coronary interventions in bifurcation lesions.

**Corresponding author: Cardiovascular Science Division of the NHLI within Imperial College of Science, Technology and Medicine, South Kensington Campus, London, SW7 2AZ, United Kingdom. E-mail: patrick.w.j.c.serruys@gmail.com*

SUBMITTED ON 09/04/2018 - REVISION RECEIVED ON 1st 06/10/2018 / 2nd 11/10/2018 / 3rd 18/11/2018 - ACCEPTED ON 22/11/2018

DOI: 10.4244/EIJ-D-18-00391

Abbreviations

BRS	bioresorbable scaffold
CT	computed tomography
DES	drug-eluting stent
EEM	external elastic membrane
FD	frequency domain
FFR	fractional flow reserve
FKBI	final kissing balloon inflation
IVUS	intravascular ultrasound
LA	lumen area
LM	left main
MLA	minimum lumen area
MSA	minimum stent area
MV	main vessel
OCT	optical coherence tomography
OFDI	optical frequency domain imaging
PCI	percutaneous coronary intervention(s)
POT	proximal optimisation technique
QCA	quantitative coronary angiography
SB	side branch
TAP	T and protrusion
TCFA	thin-cap fibroatheroma
WSS	wall shear stress

Introduction

A coronary bifurcation lesion is a lesion occurring at, or adjacent to, a significant division of a major epicardial coronary artery[1]. Coronary artery bifurcation lesions comprise approximately 15-20% of all percutaneous coronary interventions (PCI)[2] and constitute a complex lesion subgroup. Due to the complex three-dimensional structure of bifurcations causing overlapping and foreshortening, conventional angiography has an inherent limitation in the quantitative assessment of bifurcation lesions[3].

Intravascular optical coherence tomography (OCT) is a promising adjunctive tool for guiding coronary bifurcations with its unrivalled high resolution (10-20 µm) **(Supplementary Appendix 1)**. Currently, two systems are commercially available, OCT and optical frequency domain imaging (OFDI), using the same fundamental technology of optical frequency domain imaging, each with a different commercial implementation. Compared to angiography, intravascular OCT has a clear advantage in that it depicts ostial lesion(s) in bifurcation without the misleading two-dimensional appearance of conventional angiography such as overlap and foreshortening. In addition, OCT has the ability to reconstruct a bifurcation in three dimensions and to assess the side branch (SB) ostium from a three-dimensional (3D) reconstruction of the main vessel (MV) pullback.

Although all the potential benefits of adequately using the OCT information are highly appealing, its clinical value remains to be established. The currently available clinical data are based mainly on observational studies with a small number of patients **(Supplementary Table 1)**. There are as yet few prospective clinical data to suggest clinical benefits of OCT guidance for bifurcation lesions **(Supplementary Table 2)**. In the prospective randomised OPINION trial, comparing OCT and IVUS guidance in terms of patient outcome (n=829), 38% of lesions involved bifurcation[4]. However, no specific guidance protocol for bifurcation was available. In the ILUMIEN III trial, comparing IVUS and OCT guidance (n=450), bifurcation lesions requiring a two-stent strategy were excluded by protocol[5]. In the meantime, with the increasing complexity of bifurcation lesions and treatment, clinicians are more frequently implementing OCT imaging in bifurcation PCI[6]. Comparisons between OCT and IVUS in bifurcation lesions are summarised in **Supplementary Table 3**.

The European Bifurcation Club is an academic consortium created in 2004 whose goal has been to assess and recommend the appropriate strategies to manage bifurcation lesions. The Japanese Bifurcation Club was established and endorsed by the Japanese Association of Cardiovascular Intervention and Therapeutics in 2012 and shares the same aim as the European Bifurcation Club. This document provides the recommendations of the two bifurcation clubs on the OCT guiding of coronary interventions in bifurcation lesions.

– OCT may be of particular value in guiding bifurcation PCI, without the limitations of conventional angiography such as foreshortening or overlap.

Editorial, see page 1537

OCT ACQUISITION IN BIFURCATION LESIONS

Current OCT catheters (Dragonfly™ OPTIS™ [Abbott Vascular, Santa Clara, CA, USA] and Lunawave® OFDI [Terumo Corp., Tokyo, Japan]) are used with a standard 0.014-inch steerable guidewire with a monorail system. During image acquisition, typically, contrast medium is injected at a speed of 3-5 ml/s. With a pullback speed of 10-40 mm/s, image acquisition usually finishes in 5-10 seconds. Recent consoles enable an automatic detection of luminal border as well as online 3D reconstruction, which could foster the understanding of the complex anatomy of bifurcations[7,8].

In bifurcations, special attention is needed to acquire an optimal OCT image **(Supplementary Table 4)**[9]. Due to the difference in diameter of distal and proximal vessels, the scan range should be adjusted according to the size of the proximal vessel. The evaluation of a side branch ostium is often of interest; however, the guidewire shadow can hide the ostium partially or entirely. In such a case, repeat pullback after manipulation of the guidewire may be required. The nature of the bifurcation should be taken into account, including the tapering of the vessel according to conservation of flow and plaque distribution, especially on the opposite side of the carina. Predilatation of the SB is often necessary for successful OCT acquisition in the SB.

CO-REGISTRATION OF OCT AND ANGIOGRAPHY

The recent OCT consoles can co-register optical cross-section images with cineangiography acquired during a pullback, by automatic detection of the radiopaque marker of the optical lens on cineangiography. Practically, it is essential to acquire the cineangiography during the whole pullback, starting angiographic acquisition just before the start of pullback. In a complex bifurcation

lesion, it is often a challenge to co-register OCT and angiography accurately due to the overlap and foreshortening of bifurcation anatomy on angiography[3]. It is important to select the angiographic view with the best visualisation of the bifurcation with minimal overlap and foreshortening.

The online co-registration could help the operator to position a stent in a precise landing zone according to the OCT finding, and potentially reduce the risk of geographic miss as well as subsequent adverse outcomes[10,11]. The DOCTOR fusion study, comparing frequency domain (FD)-OCT guidance and angiographic guidance in general PCI, demonstrated that, in the absence of such a co-registration, the target lesion (plaque) indicated by FD-OCT was not fully covered by the implanted stent in approximately 70% of cases[10,12]. Although co-registration may be of help in stent positioning, it should be noted that eventually the stent needs to be deployed using angiographic guidance alone.

– Use of online co-registration of OCT and angiography may facilitate the precise guidance of bifurcation PCI.

THREE-DIMENSIONAL OCT IN BIFURCATION

The application of 3D reconstruction of the coronary bifurcation has been described previously[8]. With two-dimensional (2D) imaging it is difficult and not always feasible to visualise the complex anatomy of the bifurcation and the effects of intervention. With 3D OCT it is easier to recognise the anatomical changes after intervention than with 2D OCT. For example, in the endoscopic 3D view of the coronary artery, it was clearly demonstrated that after stenting in the MV the carina was shifted towards the side branch, creating a stenosis at the ostium **(Supplementary Figure 1)**[13].

ONLINE AND OFF-LINE SOFTWARE FOR 3D OCT

Recently, 3D reconstruction has become feasible online. The ILUMIEN™ Optis™ system (Abbott Vascular) has a 3D bifurcation mode, in which software automatically recognises the carina as well as side branch ostia with a diameter of ≥1.5 mm. With automatic stent enhancement, the recrossing point in bifurcation is depicted in a 3D view **(Figure 1)**. In a "stent roadmap" view, the lumen profile reconstructed from automatic lumen delineation allows a superimposition of malapposed struts[14]. The Terumo OFDI console has online software of 3D imaging with stent enhancement, which enables online reconstruction within one minute **(Figure 2)**[14].

The Medis company (Leiden, the Netherlands) has developed a dedicated OCT software, in which 3D angiography and OCT are co-registered. In addition, this software enables quantitative assessment of the side branch ostium by using an OCT pullback from the main branch (MB) in a cross-section which is perpendicular to the side branch centreline[15]. For precise sizing of a side branch ostium, OCT pullbacks could be performed in both the MV and SB, which is often challenging in clinical practice due to safety concerns including the use of an excessive amount of contrast media. Although OCT assessment in SB OCT pullback remains the gold standard, measurements of the side branch ostium performed online by cut-plane analysis of an OCT pullback of the MV have a high correlation with reference measurements performed in an SB OCT pullback and also lower errors compared with conventional analysis[15]. Use of such software is preferable since the insertion of the OCT catheter through the MV struts into the side branch is not always easy, may deform the stent and implies additional contrast medium **(Figure 3)**.

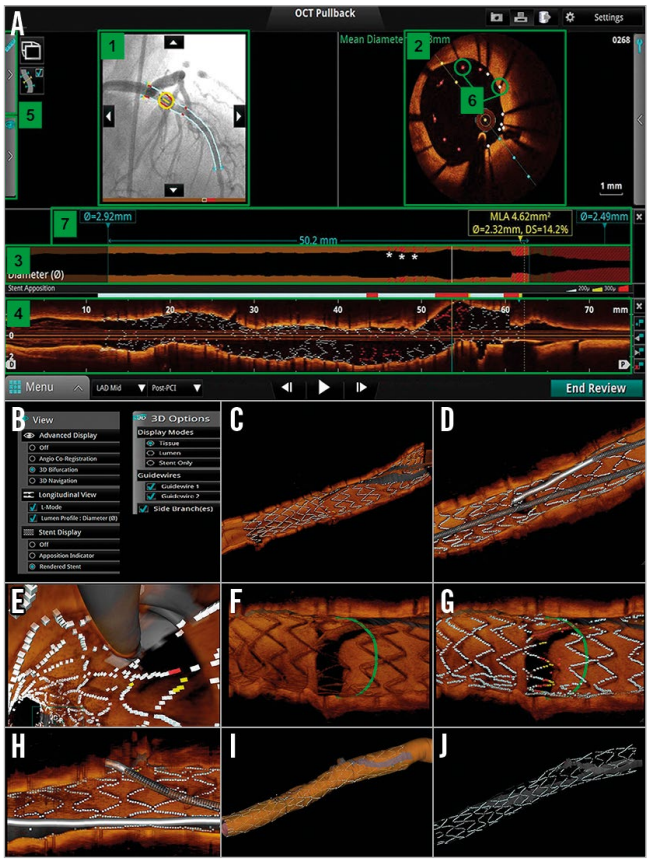

Figure 1. *Overview of online 3D reconstruction. A) "Stent roadmap" indicates the location of the minimal lumen area and suggests the proximal and distal landing zones for the stent placement based on the mean lumen area measurements. At the same time bookmarks are provided on the co-registered angiogram to assist in the overall orientation. 1) Angio co-registration, 2) cross-sectional view, 3) lumen profile view, 4) longitudinal view, 5) fold-out tabs, 6) apposition indicators, 7) stent roadmap, *) invalid frame. Panels B to J represent an overview of online 3D OCT images reconstructed by the ILUMIEN™ Optis™ system (Abbott Vascular). B) In the dedicated panels for 3D reconstruction, the particular options such as "view" (i.e., longitudinal, stent display) and "display" (i.e., stent, tissue, lumen, and guidewires) are available for several types of 3D image. C) 3D navigation view with stent display. D) 3D navigation view with stent and guidewires. E) 3D navigation view (fly-through) with stent and guidewires. F) 3D bifurcation view with tissue display. G) 3D bifurcation view with stent display. H) 3D bifurcation view with stent and guidewires. I) 3D navigation view with lumen display mode. J) 3D navigation view only with stent display. (Reproduced from OCT Atlas, 2nd edition)*

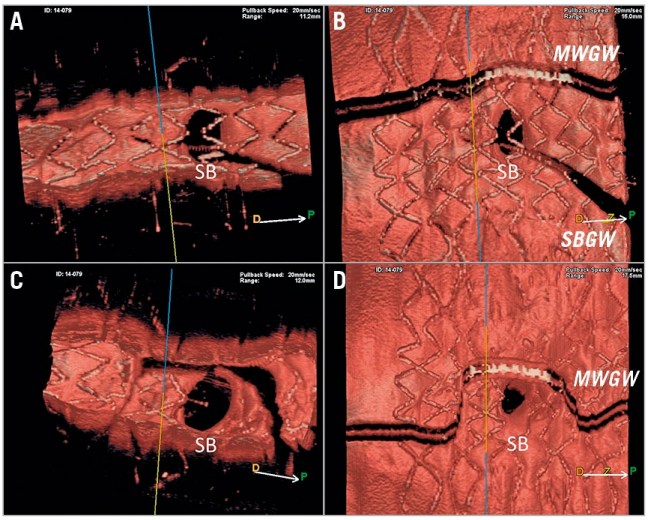

Figure 2. *Online 3D reconstruction images by OFDI. Online 3D images reconstructed by OFDI (Lunawave® system; Terumo, Tokyo, Japan) are shown. A) Vessel view before kissing balloon dilatation (KBD). B) Carpet view before KBD. C) Vessel view after KBD. D) Carpet view after KBD.*

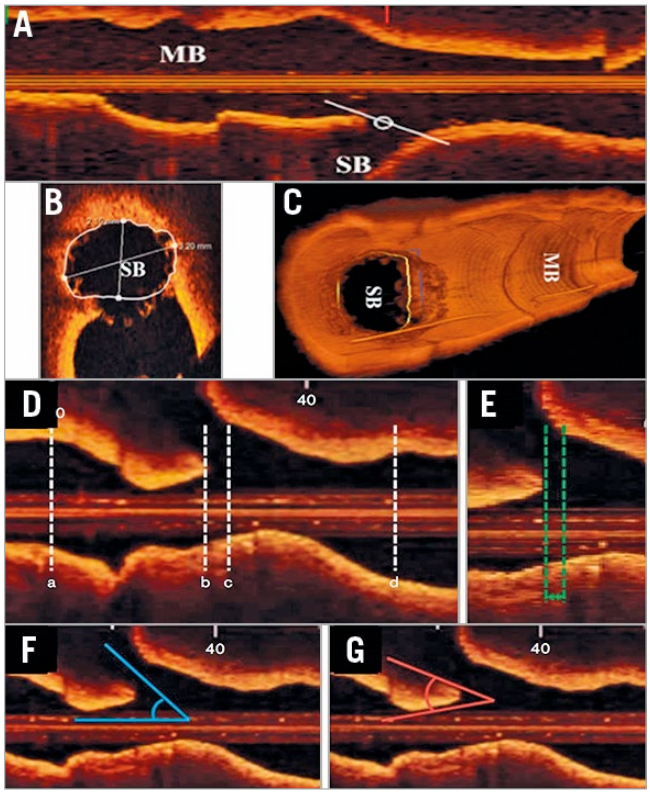

Figure 3. *Analysis using reconstructed OCT images: cut-plane analysis using pullback from MV and angle measurement in side branch in longitudinal view. A) Measurements of the SB ostium can be performed in the main branch (MB) pullback (B) by cut-plane analysis. C) The 2D cross-section is adjusted to capture the true vessel morphology perpendicular to the SB centreline. Modified from Karanasos et al[15]. For angle measurement in the side branch (D), the specific longitudinal reconstruction image was determined when both carina and the SB ostium could be identified clearly, as well as showing the narrowest carina angle: (a) distal reference site, (b) carina tip, (c) proximal branching point, (d) proximal reference site. E) The length between the proximal branching point and the carina tip (BP-CT length). F) Side branch angle (SB angle). G) Carina tip angle (CT angle). Modified from Watanabe et al[36].*

Quantitative assessment on 3D OCT is commonly used in clinical trials **(Supplementary Table 5)**. The CAAS IV-LINQ software (Pie Medical, Maastricht, the Netherlands) provides the real-time co-registration of angiography with intravascular imaging, while CAAS IntraVascular software enables 3D reconstruction of the SB ostium on OCT.

– Whenever available, use of online 3D reconstruction is recommended to facilitate the understanding of complex coronary anatomy and device-vessel interaction during bifurcation PCI.
– Unlike with IVUS, 3D assessment of the ostial area from OCT pullback of the MV is a good substitute for a pullback from the SB.

PREPROCEDURAL LESION ASSESSMENT

Preprocedural assessment of lumen and plaque distribution in bifurcation on OCT may provide essential information on treatment indication and planning of bifurcation PCI. Although the functional assessment of stenosis is a standard of care for angiographically intermediate lesions, interpretation of fractional flow reserve (FFR) results is challenging, for example, in a bifurcation lesion with proximal stenosis, or downstream stenosis due to the so-called "branch-steal" phenomenon[16]. There are several cut-off criteria of OCT-derived minimum lumen area (MLA) to predict significant FFR; however, such a threshold should be used considering the distal myocardial mass beyond each branch of the bifurcation lesion. In other words, there is no single threshold to be used[17-19]. Conversely, functional assessment without anatomical information cannot predict the anatomical changes after stenting (e.g., carina shift), which is essential for bifurcation PCI planning.

Atherosclerotic change in bifurcation is influenced by distribution of wall shear stress. Coronary plaque was mostly present in low wall shear stress (WSS) regions[20]. In bifurcation lesions, plaque grows from the outer wall (low WSS) of the bifurcation towards the flow divider (high WSS). These findings were confirmed in an OCT study[21], demonstrating that thin-cap fibroatheroma (TCFA) was localised predominantly in the region opposite the flow divider, whereas the flow divider was rarely affected. Lipid accumulation tends to develop in the zone opposite the side branch. In a multi-modality assessment of bifurcation with IVUS virtual histology and OCT, the proximal rim of the ostium of the side branch was identified as a region more likely to contain thin fibrous cap and a greater proportion of necrotic core[22-24]. However, it remains to be demonstrated how we can integrate this information to guide bifurcation intervention.

Assessment of calcification by OCT could indicate which lesion preparation should be performed. Since calcification does

not scatter light, OCT could evaluate the circumferential extension and the depth (superficial vs. deep) of calcification. In general, extensive calcification on OCT is associated with suboptimal stent expansion, stent malapposition, and failure of device delivery[10,25-30]. The latter may be especially important for the delivery of a dedicated bifurcation device or bioresorbable scaffold with a large profile. For superficial and/or circumferential calcification, atherectomy using a rotablator or orbital atherectomy system may be preferred, whereas deep calcification may preferably be treated with a cutting or scoring balloon through incisions between calcified and non-calcified plaque[10,31-34]. However, whether the information on calcium by OCT may be used to select specific strategies aimed at improving final results still remains unproven.

OCT assessment of the preprocedural bifurcation angle could be derived from OCT pullback in the MV. The carina tip angle is measured in a longitudinal view of OCT of the MV pullback as an angulation of the proximity of the carina **(Figure 3G)**. It has been demonstrated that the OCT-derived bifurcation angle has a good agreement with the computed tomography-derived bifurcation angle (mean bias=2.6, SD=11.4°)[35]. The preprocedural carina tip angle as assessed on OCT has an impact on side branch complication and strut coverage after stenting. The OCT study by Watanabe et al demonstrated that a carina tip angle less than 50° and a branching point-carina tip length less than 1.70 mm were independent predictors of side branch complication after MV stent implantation[36]. In the side branch ostium region, a significant negative correlation was found between the uncovered strut percentage and OCT-derived branching angle ($r=-0.41$, $p=0.0024$; $r=-0.33$, $p=0.0167$, respectively)[35].

– In preprocedural OCT, assessment of plaque distribution, calcification and lipidic plaque is important in planning the stenting strategy. Special attention should be paid in case of a narrow carina tip angle (<50°) as assessed on OCT.

EEM VS. LUMEN MEASUREMENT FOR CHOICE OF STENT SIZE

It remains controversial whether lumen area (LA)-based measurement or external elastic membrane (EEM)-based measurement should be used as a sizing parameter. Due to the aforementioned limited penetration depth of OCT, visualisation of the external elastic lamina (EEL) is often not possible – especially in a large coronary vessel with significant plaque burden, or in a vessel with a lipidic plaque[37]. The presence of lipid or macrophage in a superficial layer of plaque could also hinder the visibility of deep plaque by OCT, because both lipid and macrophage scatter and attenuate the OCT light[38]. As a result, vessel area and plaque area, which have been used for IVUS guidance, are not always available with OCT measurement.

In the recent randomised trials comparing IVUS and OCT (OPINION and ILUMIEN III), lumen-based and EEM-based algorithms were developed **(Figure 4)**. In the OPINION trial[4], the reference site was set at a cross-section adjacent to the target lesion that was most normal looking and free of lipid plaque (defined as a signal-poor region with a diffuse border). Then, the stent diameter was decided by measuring the lumen diameter at the proximal and distal reference sites, and stent length was decided by measuring the distance from the distal to proximal reference sites. In ILUMIEN III[5], the mean of EEL diameters at the proximal and distal references was measured and the smallest of these diameters was rounded down to the nearest 0.25 mm to determine the stent diameter. When the EEL could not be visualised, the proximal and distal reference lumen diameters were used. The investigators identified EEL in >180° of vessel circumference in 84% of cases, whereas the core lab reported the assessability of 95%. The EEL-based criteria were used in approximately 70% of cases, compared to the lumen-based criteria in 30%[5]. By using the EEL-EEL measurements on OCT, equal stent expansion indices between IVUS and OCT were demonstrated[5]. In the OPINION trial, the lumen area-based algorithm led to consistently lower stent sizes and minimum stent area (MSA) in the OCT group than in the IVUS group[39-41]. However, in both studies, the clinical impact of the observed difference in stent expansion was not fully investigated[5,39-41].

It should be noted that both the ILUMIEN III and OPINION trials were not studies dedicated to bifurcation. In the absence of sufficient clinical data dedicated to bifurcation, both methods (EEM and lumen area-based) could be used for sizing of a bifurcation lesion. It is important to avoid as a landing zone a segment with a large plaque burden or with a lipidic plaque. Whenever the vessel, especially the proximal vessel, is too large to measure the vessel area despite the maximal scan range, the lumen area-based algorithm is recommended.

In a bifurcation lesion, it is of importance to select a size of stent and to form the stent according to the tapering of the bifurcation, in order to restore fractal geometry with the law of flow conservation[42]. The choice of stent size should therefore be based on measurement of the reference site(s) in the proximal MV, the distal MV and/or the distal SB according to the stenting strategy. As previously recommended by EBC consensus, the MV stent should be sized according to the distal MV reference diameter, whereas the MV stent should allow for expansion to the reference diameter of the proximal MV[2].

– Either external elastic membrane areas or lumen areas can be used for sizing of the vessel. Whenever the proximal vessel is too large to measure the EEM, stent sizing according to lumen area measurement is recommended **(Figure 4)**.
– The size of stent should be selected aiming at the fractal geometry of bifurcation according to the law of flow conservation. The MV stent should be sized according to the distal MV reference diameter, whereas the MV stent should allow for expansion to the reference diameter of the proximal MV[2].

LENGTH AND POSITIONING OF STENT IN BIFURCATIONS

In terms of stent length evaluation on OCT, the operator should aim to cover the bifurcation stenosis segment at least 6-8 mm from the proximal stent edge to the bifurcation carina, to enable the appropriate proximal optimisation technique (POT) with the

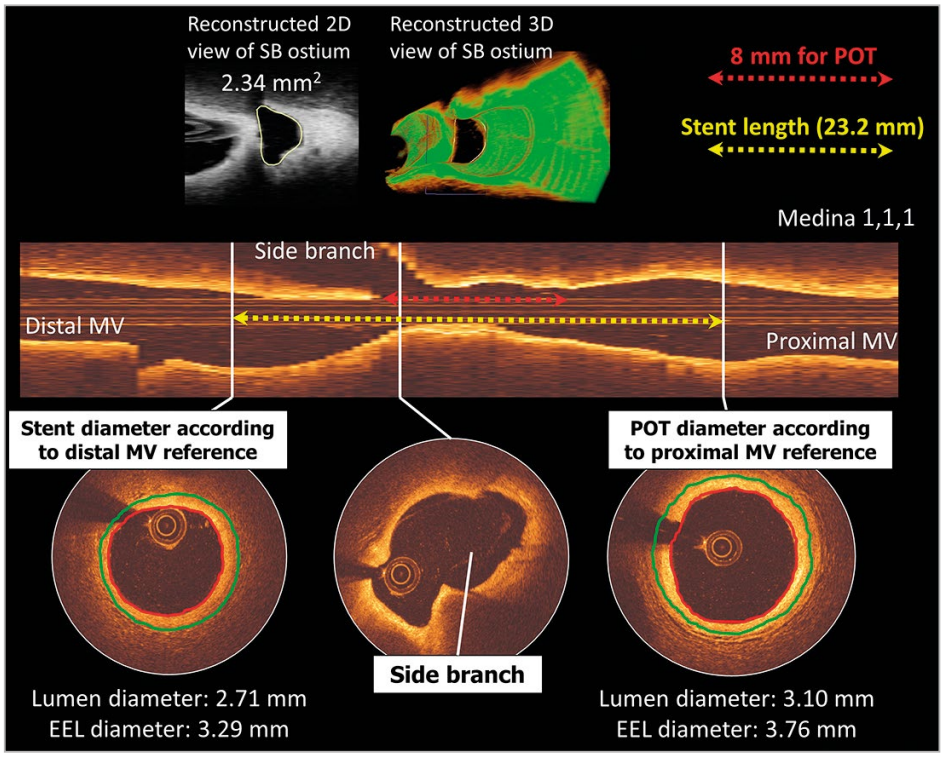

Figure 4. *Lumen-based or EEL-based guidance for stent sizing. A distal RCA bifurcation with distal and proximal reference cross-sections is shown. According to the lumen-based stent sizing used in the OPINION trial, the lumen-guided stent diameter is calculated as 2.75 mm (0–0.25 mm greater than the lumen diameter at the distal reference site). On the other hand, the smallest EEL diameter from both distal and proximal reference segments is 3.29 mm (distal reference). According to EEL-based sizing used in the ILUMIEN III trial, this was rounded down to the nearest 0.25 mm and thus a 3.25 mm diameter stent will be chosen. Stent length was decided as 24 mm by measuring the distance from the distal to the proximal reference site (yellow arrow). The operator should aim to cover the bifurcation stenosis segment at least 8 mm from the proximal stent edge to the bifurcation carina (red arrow) considering the available length of the balloon for POT. EEL: external elastic lamina; MV: main vessel; POT: proximal optimisation technique; RCA: right coronary artery*

shortest available balloon when indicated **(Figure 4)**[2]. POT is currently recommended just after implanting the stent with the distal MV diameter, whatever complementary technique may be used. In bench testing it was demonstrated that POT significantly reduced SB ostium strut obstruction, from 34.0% to 26.0%, concomitantly increasing the distal cell area ratio from 22.1% to 28.7% ($p<0.05$)[43]. As mentioned above, use of co-registration of OCT and angiography should facilitate the execution of precise stent positioning according to OCT findings.

– As far as the stent length is concerned on OCT, the operator should aim to cover the bifurcation stenosis segment at least 6-8 mm from the proximal stent edge to the bifurcation carina to enable subsequent POT with a short balloon.

DECISION MAKING ON STENTING STRATEGY USING OCT

According to the latest EBC recommendation[6], the provisional SB stenting strategy is considered the "standard" approach for treatment of the vast majority of bifurcation lesions. Upfront use of two stents may basically only be needed in very complex lesions with large calcified side branches with ostial disease extending >5 mm from the carina and in bifurcations with side branches whose access is particularly challenging and where the SB should be secured by stenting once accessed.

Following this recommendation, OCT from the SB could be used to evaluate the distribution of the calcified lesion in the side branch. In the presence of a severe ostial lesion in the SB, blood clearance is sometimes incomplete for obtaining clear OCT images in the SB. Therefore, predilatation with a small balloon may be required.

GUIDANCE OF THE REWIRING IN A DISTAL CELL OF THE STENT OVERHANGING A SIDE BRANCH OSTIUM

After placing the stent in the bifurcation using either a one-stent or two-stent technique, kissing balloon inflations are used in order to form the stent in bifurcation fractal geometry[2]. To minimise the risk of struts being pushed inside the MV by kissing balloon inflation by creating a so-called *de novo* "metal carina" in the MV, it is important to rewire in the distal cell of the jailed side branch ostium **(Figure 5)**[2]. The protrusion of the metal carina into the MV is determined mainly by the recrossing point. In general, distal recrossing promotes a better ostial side branch stent coverage and apposition, while proximal recrossing results in unusual strut deflection, a lower

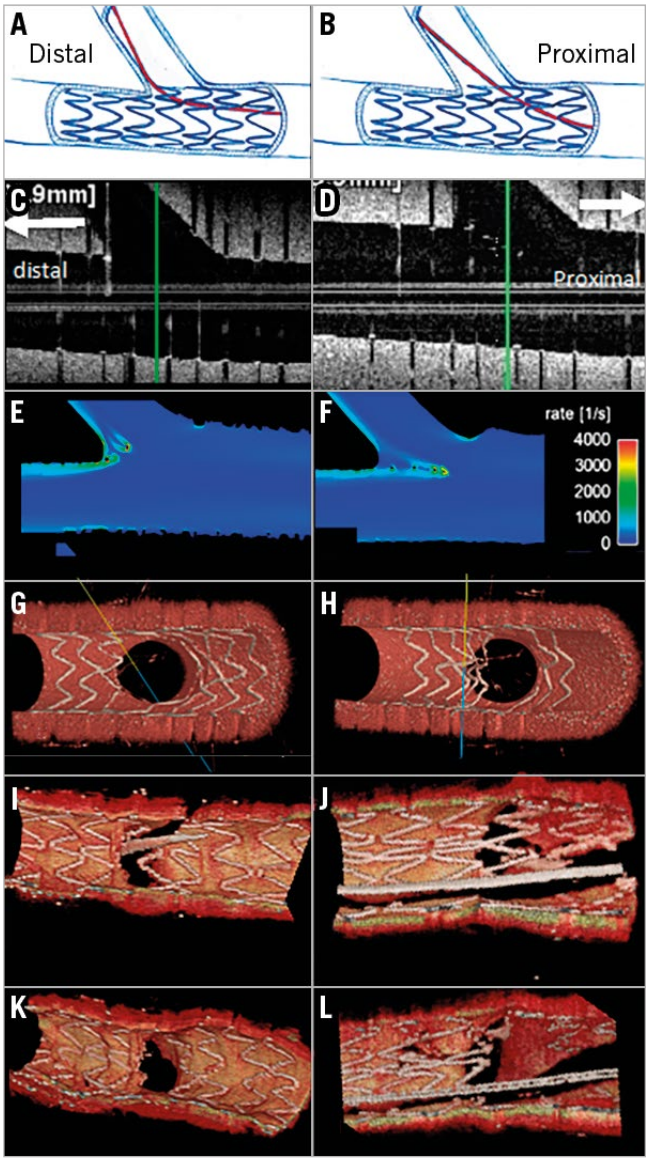

Figure 5. *Impact of the rewiring position and strut malapposition in bifurcation. Left column (A, C, E, G, I and K) and right column (B, D, F, H, J, L) show distal rewiring and proximal rewiring, respectively. Panels C and D are longitudinal OFDI images. The computational flow simulation of the shear rate is shown in panels E and F. Panels G and H show the 3D reconstruction of struts in phantom. Panels I and J indicate the wiring position in 3D OCT in human coronary bifurcation before kissing balloon dilatation (KBD), whereas panels K and L are 3D reconstruction images after KBD.*

strut coverage of the side branch ostium and more overhanging metal into the SB, resulting in a high shear rate region at the overhanging struts and a low shear rate behind them **(Figure 5)**[44].

The optimal position of wire recrossing after MV stenting is influenced not only by the distal position of the wire but also by the stent design and configuration of jailing struts[45,46]. The presence of a longitudinal link between the rings in front of the ostium was associated with more frequent malapposition compared to the cases without a longitudinal link **(Supplementary Figure 2)**.

Taking into account the design of stent, the presence or absence of a strut link in front of the ostium and the distal positioning of the recrossing wire, the proposed optimal wire position is presented in **Figure 6** (modified from Okamura et al[45]). In principle, the optimal recrossing point is in the distal compartment delineated by the bifurcation carina (yellow in **Figure 6**, panels A, A') and the most distal ring of the stent within the bifurcation. When the most distal stent ring is in contact with the rim of the carina (**Figure 6**, panels B, B'), a second distal compartment is considered the optimal cell to be recrossed with a wire. In the presence of multiple second distal compartments (**Figure 6**, panels C, C'), a larger compartment should be selected.

The feasibility of OCT guidance in selecting the recrossing point (with either 2D or 3D images) and its potential benefit have been assessed in a few studies **(Supplementary Table 1)**. Alegria-Barrero et al[47] reported that, in 52 patients undergoing elective treatment of bifurcation lesions using provisional stenting as the default strategy, lesions that were recrossed with OCT guidance (n=12) had a significantly lower number of malapposed stent struts, especially in the quadrants towards the SB ostium (9.5% [7.5-17.4] in the OCT-guided group vs. 42.3% [31.2-54.7] in the angiography-guided group, p<0.0001). In this study, OCT guidance was based mainly on 2D cross-sections. In a prospective registry with 3D OCT acquisition in bifurcation, Okamura et al demonstrated that the feasibility of assessment of the guidewire recrossing point after MV stenting was 89.9% **(Figure 7)**[45,48,49]. However, the evidence stemming from these two studies is limited to mechanistic observation.

While randomised trials such as DOCTOR Recross, OCTOBER and OPTIMUM **(Supplementary Table 2)** are ongoing to investigate the clinical benefit of online 3D OCT guidance in bifurcation treatment, it is recommended that 3D OCT imaging on the recrossing position after main vessel stenting is performed before final kissing balloon, to ensure the optimal position of the wire. The repeated 3D OCT imaging should be performed cautiously taking into account the cumulative amount of contrast agent.

– Prior to kissing balloon after stenting, it is important to recross the side branch ostium strut cell with a wire in the most distal cell to minimise the risk of pushing struts towards the MV.
– Use of OCT is recommended to exclude accidental abluminal rewiring and to assess the position of the recrossing wire. On 3D OCT, the optimal recrossing point is in the distal compartment without compromising the bifurcation carina **(Figure 6)**. When the wiring position is not optimal, repositioning of the wire may be considered **(Figure 7)**.

POST-PROCEDURAL ASSESSMENT (STENT EXPANSION, DISSECTION, MALAPPOSITION, TISSUE PROTRUSION, SIDE BRANCH OSTIUM)

After PCI in a bifurcation, OCT is used to evaluate stent underexpansion, malapposition, tissue protrusion, dissection, geographic miss and thrombus[50]. Stent expansion is evaluated either as an absolute measurement of the minimum stent cross-sectional area or as a relative expansion compared with the predefined reference

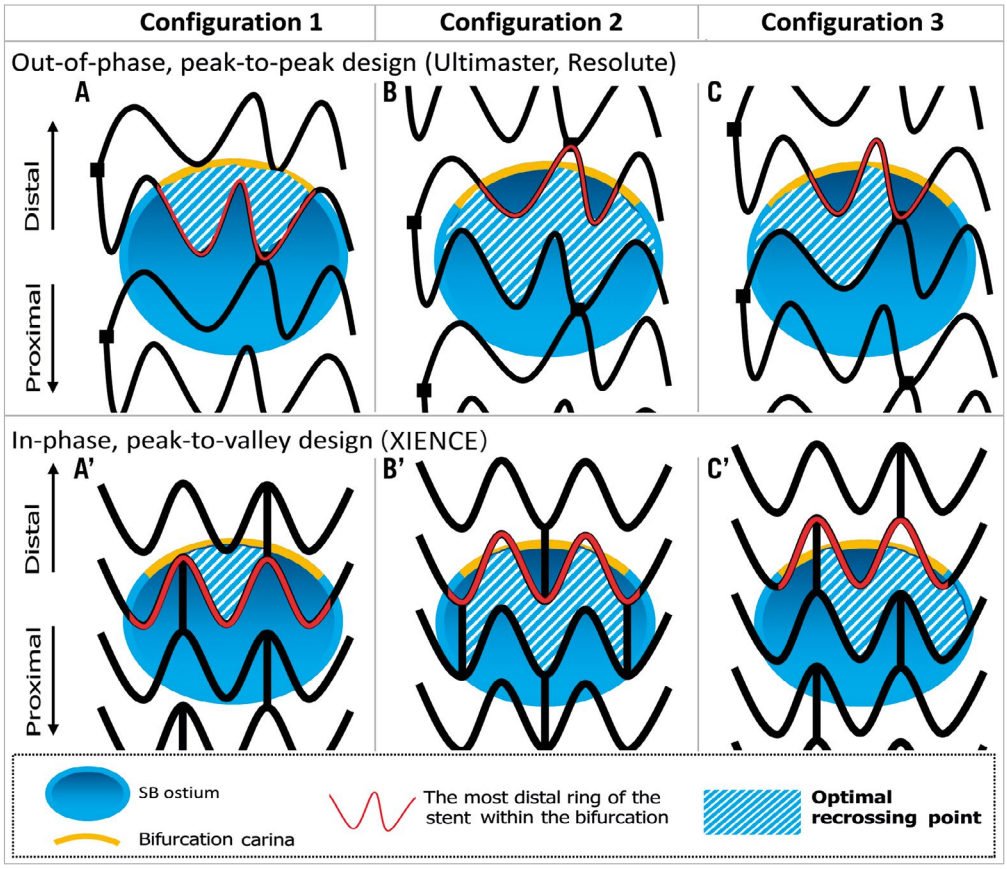

Figure 6. *Optimal recrossing point in the side branch ostium according to different configurations of overhanging struts. The upper row depicts struts with out-of-phase, peak-to-peak design placed on the side branch ostium. The lower row depicts struts with in-phase, peak-to-valley design placed on the side branch ostium. In principle, the optimal recrossing point is in the distal compartment delineated by the bifurcation carina (yellow line) and the most distal ring of the stent within the bifurcation (red strut) (configuration 1: A and A'). When the most distal stent ring is in contact with the rim of the carina (configuration 2: B and B'), a second distal compartment is considered as the optimal cell to be recrossed with a wire. In the presence of multiple second distal compartments (configuration 3: C and C'), a larger compartment should be selected.*

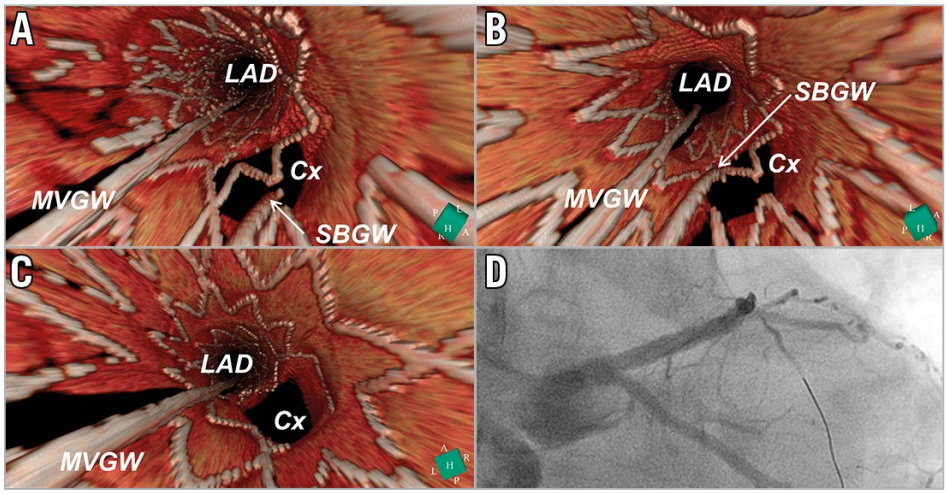

Figure 7. *Confirmation of the recrossing position of the wire after stent implantation by 3D OCT image. A metallic stent (Nobori 3.5/18 mm; Terumo) was implanted from the LM to LAD crossing over the LCx. OCT was performed after wire recrossing. 3D OCT images revealed that the position of the wire was located in the proximal cell (A). After a second attempt at rewiring, the distal recrossing was confirmed by 3D OCT (B). No malapposed struts were observed after KBD (C). Coronary angiography after KBD is shown in panel D.*

area. In a bifurcation, considering its fractal anatomy, stent expansion should be evaluated separately in the proximal MV, distal MV and SB, with respect to each reference area[51]. Larger stent expansion is generally associated with better clinical outcomes. It has been demonstrated that stent malapposition is more common at the proximal MV and tissue prolapse or dissection at the distal MV segment. In addition, previous studies have demonstrated the feasibility of 3D OCT for correction of eccentricity in the ostium area of the side branch[3,15,52-54]. In patients with complex bifurcation stenosis undergoing PCI with a dedicated bifurcation system, FKBI is associated with improved anatomical and functional results at the SB ostium, without compromising the result at the MB[55].

In general, a small edge dissection found on OCT which is undetected on angiography most likely does not have a clinical impact[56-59]. However, the following factors need to be considered: the longitudinal (≥3 mm) and circumferential extension (≥60 degrees) of the dissection, the intra-dissection lumen area respective to the reference (<90%) and the depth of the dissection (media or even adventitia). In ILUMIEN III, edge dissections were categorised as major if they constituted ≥60 degrees of the circumference of the vessel at the site of dissection and/or were ≥3 mm in length. In that trial, when the intra-dissection lumen area was <90% of the respective reference area, additional stent implantation was considered. In the CLI-OPCI II trial, dissection was defined on OCT as a linear rim of tissue with a width of ≥0.2 mm and a clear separation from the vessel wall or underlying plaque. In this retrospective multicentre registry, the acute dissection in the distal stent edge was an independent predictor of major adverse cardiac events[60].

So far, no specific study on bifurcation is available covering this aspect. If the malapposition distance from the endoluminal lining of the strut to the vessel wall is <250 µm, such struts are likely to come into contact with the vessel wall at follow-up. Therefore, such small malapposition may be less relevant[61-63]. The clinical relevance of acute malapposition on stent failure has not yet been fully established[60,64-66]. Acute strut malapposition could persist (persistent malapposition) or resolve at follow-up (resolved malapposition), whereas strut malapposition could also develop during follow-up (late acquired malapposition). The temporal evolution and disappearance of malapposition has made the investigation of the clinical relevance of strut malapposition more complicated.

– The proximal MV is predisposed to more frequent malapposition whereas the distal MV is predisposed to more frequent tissue prolapse.
– Acute incomplete stent apposition with a distance of ≤300 microns is likely to be resolved at follow-up. Additional post-dilatation is considered when the malapposition distance is >300 microns with a longitudinal extension ≥1 mm.
– Most edge dissection detected on OCT is clinically silent, whereas additional stenting may be performed if the width of the distal edge dissection is ≥200 microns[60].

LEFT MAIN BIFURCATION

Acquisition of OCT images in the left main (LM) trunk is challenging; documentation of the ostial region is in principle impossible due to cannulation of the guiding catheter beyond the ostium. Even if the guiding catheter is withdrawn from the ostium, image acquisition is difficult due to incomplete elimination of red blood cells in the aorta. In the current European guidelines for myocardial revascularisation, OCT is not considered for LM intervention, whereas IVUS is recommended as class IIa for this indication[67].

Nevertheless, a few studies have demonstrated that frequency domain OCT for sizing in the non-ostial LM coronary artery is feasible[68,69]. In 54 patients with non-ostial LM disease, Burzotta et al demonstrated that 81% of frames were analysable and that the majority of non-analysable, artefact frames were in the proximal LM[69]. In the recent IDEAL-LM trial randomising XIENCE (Abbott Vascular, Santa Clara, CA, USA) and SYNERGY™ (Boston Scientific, Marlborough, MA, USA) stents in LM lesion PCI, post-implantation FD-OCT results were available in 91% of lesions.

In a study by Fujino et al, post-procedure, malapposed struts were more frequently observed in the proximal segment of the LM treated with drug-eluting stents, compared to the distal segment. At nine months, malapposition and uncovered struts were also more frequently observed in the proximal segment[70]. Taking into account the physiological significance of overhanging struts in front of the circumflex ostium or LAD ostium, the importance of 3D OCT guidance for the recrossing point through the cell strut is also emphasised in LM stenting **(Figure 7)**. In the randomised EXCEL trial, acute LM stent deformation assessed by IVUS was most frequently observed in the LM ostium (5.4%) and was associated with a higher lesion failure (HR 2.15, 95% CI: 1.05, 4.40, p=0.04). On OCT, longitudinal measurement as well as 3D reconstruction is useful to detect the longitudinal deformation, although OCT is limited in the assessment of an ostial lesion.

In post-procedural evaluation, an IVUS study suggested certain cut-offs for minimal lumen areas after left main stenting[71]. Similar cut-offs using OCT still need to be validated; however, considering that OCT provides slightly smaller yet comparable corresponding measures, the values may safely be applied with OCT as well[9].

– In interventions of non-ostial LM disease, OCT guidance is feasible and may be considered as long as the proximal stent edge is not covering the LM ostium.

OCT TO EVALUATE BIFURCATION-DEDICATED STENTS AND NEW TECHNOLOGIES

OCT has also been used to assess the procedural success of new bifurcation stenting technologies and bioresorbable scaffolds **(Supplementary Appendix 2-Supplementary Appendix 7, Supplementary Figure 3-Supplementary Figure 5)**. Most case reports visualise the complex anatomical structure of bifurcation-dedicated stents in 3D OCT **(Supplementary Table 6)**. There are also several studies reported **(Supplementary Table 7)** or ongoing **(Supplementary Table 8)** with endpoints defined by OCT measurements.

– OCT is used to assess the acute and chronic efficacy of a dedicated bifurcation stent system. 3D OCT facilitates the understanding of the device structures *in vivo*.

Conclusion

This consensus document is based on expert opinion of the members of the European Bifurcation Club and Japanese Bifurcation Club on the usage of OCT in coronary bifurcation PCI. With recent technical and technological advances, it is feasible to use OCT in guiding complex procedures in bifurcations. Although the recent clinical evidence starts to support OCT guidance, dedicated evidence for bifurcation treatment is still warranted. This document should be updated and expanded in the future according to the upcoming clinical evidence stemming from ongoing trials and investigations.

Appendix

Contributors: Pascal Motreff, MD, PhD, *Cardiology Department, CHU Clermont-Ferrand, Clermont-Ferrand, France; Cardio Vascular Interventional Therapy and Imaging (CaVITI), Image Science for Interventional Techniques (ISIT), UMR CNRS 6284, Auvergne University, Clermont-Ferrand, France*; Ricardo A. Costa, MD, PhD, *Instituto Dante Pazzanese de Cardiologia, São Paulo, Brazil;* Gérard Finet, MD, *Hôpital Cardiologique, Claude Bernard University, Lyon, France*; Yusuke Fujino, MD, PhD, *Department of Cardiology, New Tokyo Hospital, Chiba, Japan*; Juan Luis Gutiérrez-Chico, MD, PhD, FESC, FACC, *Department of Interventional Cardiology, Charité University Hospital, Campus Benjamin Franklin, Berlin, Germany*; Indulis Kumsars, MD, *Latvian Center of Cardiology, Paul Stradins Clinical Hospital, Riga, Latvia*; Massoud A. Leesar, MD, *Division of Cardiovascular Diseases, University of Cincinnati, Cincinnati, OH, USA*; Jacek Legutko, MD, PhD, *Institute of Cardiology, Jagiellonian University Medical College, Krakow, Poland*; Jasvindar Singh, MD, *Division of Cardiology, Department of Medicine, Washington University School of Medicine, St. Louis, MO, USA*; Yoshinobu Murasato, MD, *Kyushu Medical Center, Fukuoka, Japan*; Junya Shite, MD, PhD, *Department of Cardiology, Osaka Saiseikai Nakatsu Hospital, Osaka, Japan*; Yutaka Hikichi, MD, *Saga University School of Medicine, Saga, Japan.*

Guest Editor

This paper was guest edited by Adnan Kastrati, MD; Deutsches Herzzentrum München, Munich, Germany.

Conflict of interest statement

Y. Onuma is a member of the Advisory Board of Abbott Vascular. F. Burzotta has received speaker's fees from Abbott/St. Jude in relation to talks on OCT use. N. Holm reports grants and personal fees from Abbott, personal fees from Terumo, grants and personal fees from Boston Scientific, and grants from Medis medical imaging systems. N. Amabile reports honoraria and/or consulting/lecture fees from Boston Scientific and Abbott Vascular. G. Mintz reports fellowship and/or research support from Boston Scientific, Abbott and Philips, and honoraria and/or consulting/lecture fees from Boston Scientific, Philips and Infraredx. T. Lefèvre reports fees from Abbott Vascular. P. Motreff has served as a consultant for Terumo and Abbott. J. Legutko reports lecture fees from Terumo and Abbott. J. Singh has served as a consultant/speaker for Abbott and Philips/Volcano. J. Shite reports lecture honoraria from Abbott and Terumo. P.W. Serruys is a member of the Advisory Board of Abbott Vascular. The other authors have no conflicts of interest to declare. The Guest Editor has no conflicts of interest to declare.

References

The references can be found in the online version of this article.

Supplementary data

Supplementary Appendix 1. OCT in comparison to QCA and IVUS.

Supplementary Appendix 2. OCT to evaluate bifurcation-dedicated stents.

Supplementary Appendix 3. OCT for bioresorbable scaffolds.

Supplementary Appendix 4. Polymeric bioresorbable scaffolds.

Supplementary Appendix 5. Magnesium scaffold.

Supplementary Appendix 6. OCT in bench testing and preclinical study.

Supplementary Appendix 7. Flow-velocity and pressure simulation in bifurcations using OCT and 3D angiography.

Supplementary Figure 1. Carina shift in the distal right coronary artery visualised on 3D OCT.

Supplementary Figure 2. Configurations of overhanging struts in front of the side branch ostium and the results of KBD.

Supplementary Figure 3. Hybrid treatment of bifurcation lesions with BVS and metallic stents.

Supplementary Figure 4. The jailed side branch with the number of compartments created by the criss-cross of the struts as well as the configuration of the jailing struts.

Supplementary Figure 5. Serial assessment of jailed side branch over five years.

Supplementary Table 1. Published clinical studies on OCT-guided PCI in bifurcations.

Supplementary Table 2. Randomised controlled trials of OCT versus angiography-guided or IVUS-guided drug-eluting stent implantation with or without bifurcation lesions.

Supplementary Table 3. Comparison of IVUS versus OCT in bifurcation treatment.

Supplementary Table 4. OCT acquisition in bifurcations. Tips and tricks.

Supplementary Table 5. Clinical studies with qualitative or quantitative endpoints using 3D OCT.

Supplementary Table 6. Case reports of bifurcation-dedicated stents with OCT evaluation.

Supplementary Table 7. Clinical studies of bifurcation-dedicated stents with OCT evaluation.

Supplementary Table 8. Ongoing device trials in bifurcation using OCT.

The supplementary data are published online at: http://www.pcronline.com/eurointervention/148th_issue/269

Supplementary data

Supplementary Appendix 1. OCT in comparison to QCA and IVUS

OCT has the highest resolution (10-20 microns) amongst imaging modalities used in the cath lab. Flushing with contrast media (or diluted contrast/plasma expander) is required to eliminate red blood cells which scatter the light. OCT provides a clear view of the border between the lumen and the endoluminal lining of the vessel wall, which enables precise automatic lumen detection. However, due to the limited penetration of light, the assessment of the full thickness of the vessel wall is often impossible, especially in the coronary artery with atherosclerotic plaque. In general, there is an inherent difference in the measurement of lumen dimensions using QCA, IVUS and OCT. Previous studies consistently showed the following ranking in luminal dimensions assessed by these modalities: QCA<OCT<IVUS. OCT is the most accurate in lumen measurement according to the previous phantom, histomorphometric and clinical studies[72-75]. Recently, in the OPUS-CLASS study, Kubo et al confirmed this relationship of lumen dimensions assessed by OCT, IVUS and QCA in a clinical and a phantom study[76,77].

Supplementary Appendix 2. OCT to evaluate bifurcation-dedicated stents

OCT has also been used to assess the procedural success of new bifurcation stenting technologies. Most case reports visualise the complex anatomical structure of bifurcation-dedicated stents in 3D OCT **(Supplementary Table 6)**. Clinical studies with bifurcation-dedicated stents are shown in **Supplementary Table 7**. Those studies analysed strut apposition[78-83] and strut coverage[78,80,84-86] in bifurcation dedicated-stents such as BiOSS LIM (Balton, Warsaw, Poland), Tryton (Tryton Medical, Inc., Durham, NC, USA), Axxess™ (Biosensors Europe SA, Morges, Switzerland).

Ferrante et al used OCT to assess the efficacy of the Tryton dedicated side branch stent in nine patients, and found that malapposed stent struts were more frequently seen at the level of the bifurcation than in the proximal and distal stent in the MV. In particular, the highest proportion of malapposed struts was seen “towards the ostium of the side branch”[87].

Recently, the COBRA trial compared the Axxess bifurcation stent in the proximal MV and additional BioMatrix stents in the branches (Biosensors Europe SA), versus a culotte technique using XIENCE stents (Abbott Vascular, Santa Clara, CA, USA). At 9 months, the

percentages of uncovered struts were similar; however, a strategy using Axxess resulted in a significantly larger lumen in the proximal MV both acutely (minimum lumen diameter 3.03±0.51 vs. 2.71±0.44 mm, p=0.04) and at follow-up (mean lumen area 10.0±2.1 vs. 7.1±1.8 mm^2, p<0.001)[84]. These studies demonstrate that the use of OCT will be important in the development of new stenting technologies designed to challenge complex bifurcation lesions. Other ongoing device trials in bifurcation using OCT are shown in **Supplementary Table 8**.

Supplementary Appendix 3. OCT for the bioresorbable scaffold

Fully bioresorbable scaffolds (BRS) are a novel treatment approach for coronary narrowing which provide transient vessel support with drug delivery capability[73,88-90]. Currently, five products have received a CE mark (Absorb™ [Abbott Vascular], Magmaris™ [Biotronik, Bülach, Switzerland], DESolve® [Elixir Medical Corporation, Milpitas, CA, USA], Fantom® [REVA Medical, San Diego, CA, USA] and ART [Arterial Remodeling Technologies, Paris, France]), although the Absorb scaffold has been withdrawn from the market by the manufacturer.

However, the mechanical properties of the bioresorbable materials, typically poly-lactide or magnesium, are weaker than those of permanent metals (tensile strength, Young's modulus and % elongation at break). This results in a scaffold design with thicker and wider struts and a large crossing profile of the delivery system, potentially resulting in increased acute thrombogenicity[91]. These limitations of BRS warrant dedicated implantation methods, especially in bifurcation.

Supplementary Appendix 4. Polymeric bioresorbable scaffolds

Usage of polymeric scaffolds in bifurcation lesions is currently limited, mainly due to the risk of acute mechanical disruption of scaffold struts when typical bifurcation techniques are applied[2].

In an experimental bifurcation bench model with the Absorb scaffold, side branch fenestration with a 2.5 or 3.0 mm balloon and pressure >10 atm increased the risk of breaking connectors or hoops[92]. To avoid mechanical disruption due to overexpansion of the proximal part by the classic kissing balloon technique, the "snuggling" technique or "mini-kissing

balloon" technique, with minimal overlap of the balloons, is recommended[92-94].

The provisional approach remains the default strategy for treating bifurcations with a polymeric bioresorbable scaffold[94,95]. In case the provisional strategy turns into a two-device technique, the culotte and crush techniques have to be avoided to prevent excessive overlapping of the thick struts and structural deformation of the scaffold[96]. If the SB is compromised, open a cell with an undersized NC balloon (≤2.5 mm) and use POT with a larger balloon in the proximal MV to correct scaffold malapposition (the sequential strategy: POT+SB opening+final POT)[97,98].

OCT is essential to diagnose acute disruptions and late discontinuities of the polymeric BRS, since angiography and/or IVUS are not able (or limited) to detect such a complication. 3D OCT facilitates the detection of acute disruption in case of overlap in bifurcation **(Supplementary Figure 3)**. The 3D image could be used to classify the jailed side branch according to the number of compartments created by the criss-cross of the struts as well as the configuration of the jailing struts **(Supplementary Figure 4)**[55]. In serial assessment, the 3D image demonstrated the alteration of the carina due to the bioresorption process **(Supplementary Figure 5)**.

Supplementary Appendix 5. Magnesium scaffold

So far, scarce clinical data are available for bifurcation treatment using the Magmaris magnesium-based bioresorbable scaffold. Expert opinion does not recommend treatment of a bifurcation lesion with this device in the presence of a significant side branch[99]. OCT could be used as a "safeguard" to select appropriate lesions[100].

According to a recent preclinical experiment[101], bifurcation stenting using the Magmaris appears feasible, and provisional scaffolding with additional TAP whenever needed seems a reasonable approach. Whenever a two-stent technique is planned, TAP appears most favourable, whilst modified-T and culotte stenting should probably be avoided due to the increased rate of scaffold fracture.

Supplementary Appendix 6. OCT in bench testing and preclinical study

In bench testing, micro-computed tomography (micro-CT) is the gold standard for the evaluation of stents and stent techniques. OCT can be used for bench evaluation using

translucent silicone phantoms yielding results almost comparable to micro-CT. The current EAPCI task force for DES and BRS recommends OCT as a measurement of lumen area in preclinical study, since histological evaluation of the lumen is biased by shrinkage of tissue induced during the histological fixation process.

Supplementary Appendix 7. Flow-velocity and pressure simulation in bifurcation using OCT and 3D angiography

In combination with 3D angiography, OCT could provide a high-quality 3D reconstruction of coronary bifurcation, which enables computational flow dynamics, simulation of flow velocity and pressure (fractional flow reserve)[102]. Although further technological development is warranted, online simulation of shear stress and pressure drop in bifurcation lesions could potentially improve the treatment approach to bifurcation lesions. Ongoing studies such as the FORECAST trial will further inform us as to the clinical impact of this new combined methodology.

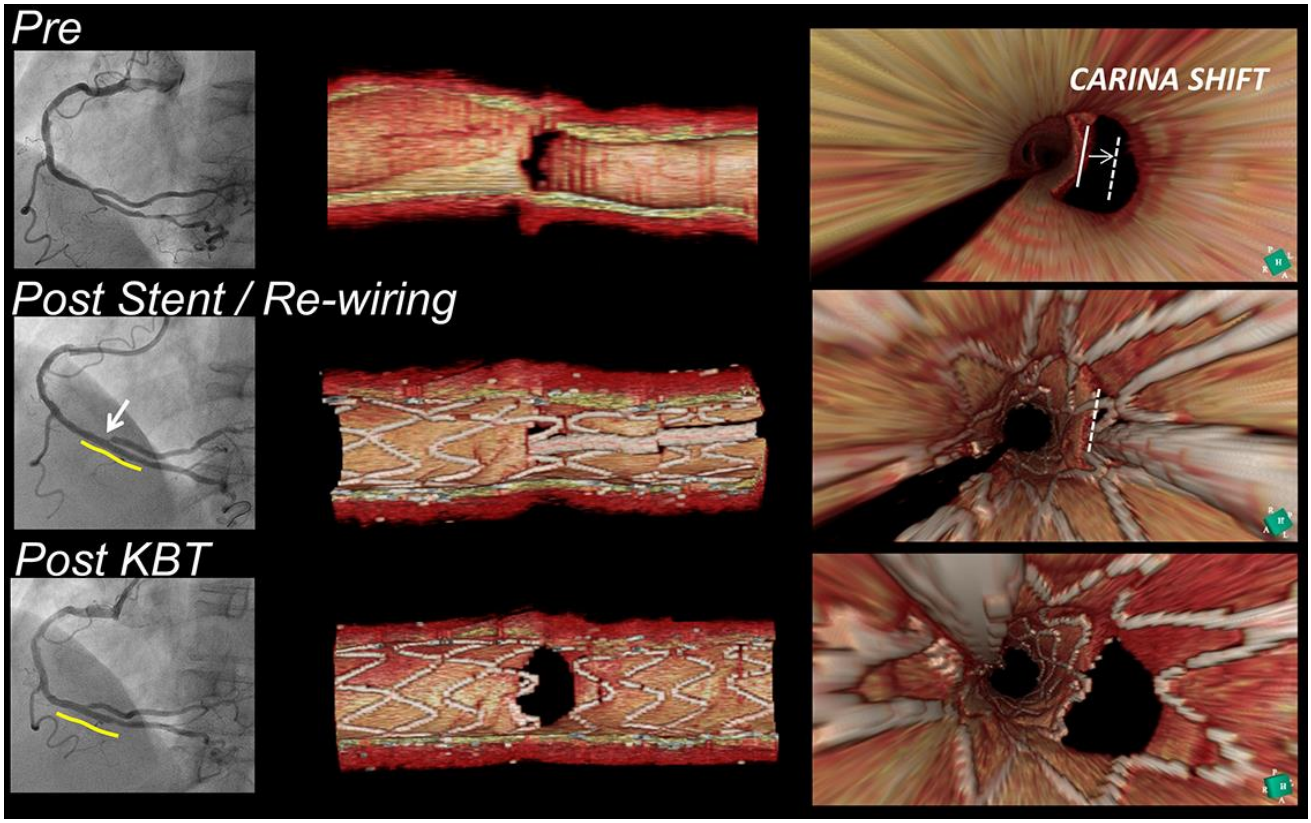

Supplementary Figure 1. Carina shift in the distal right coronary artery visualised on 3D OCT. After implantation of the Resolute Integrity (2.5/18 mm) stent (Medtronic, Minneapolis, MN, USA) in #3-#4PD, a carina shift was observed in 3D OCT images (white arrow). The kissing balloon technique was performed, followed by the dilatation of the side branch orifice seen in both 3D OCT and coronary angiography.

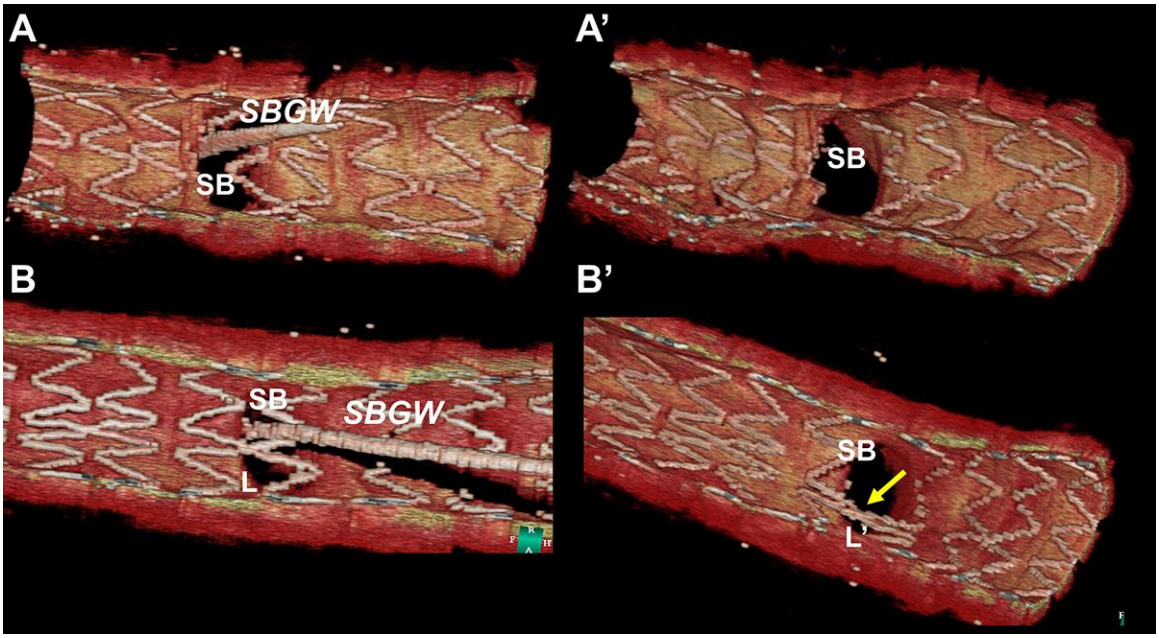

Supplementary Figure 2. Configurations of overhanging struts in front of the side branch ostium and the results of KBD.

In free carina type configuration with distal rewiring (A), no ISA was observed in front of the side branch ostium (A'). In the connecting to carina type configuration, even though distal rewiring was achieved (B), malapposed struts were detected (B').

A) LMT-LAD, SB LCX, Resolute Integrity 2.5-22 mm (Medtronic, Minneapolis, MN, USA), Link(-), distal rewiring.

A') KBD (2.5 mm stent balloon for MV, Glider™ balloon 2.0 mm [QT Vascular Ltd, Singapore]), POT 3.5 mm ballooning.

B) LAD mid, diagonal, after deployment of Nobori 3.5-18 mm (Terumo, Tokyo, Japan), Link(+), distal rewiring.

B') LAD mid, diagonal, after KBD (MV 3 mm, SB 2 mm).

ISA: incomplete stent apposition; L, L': link, SB: side branch; SBGW: side branch guidewire

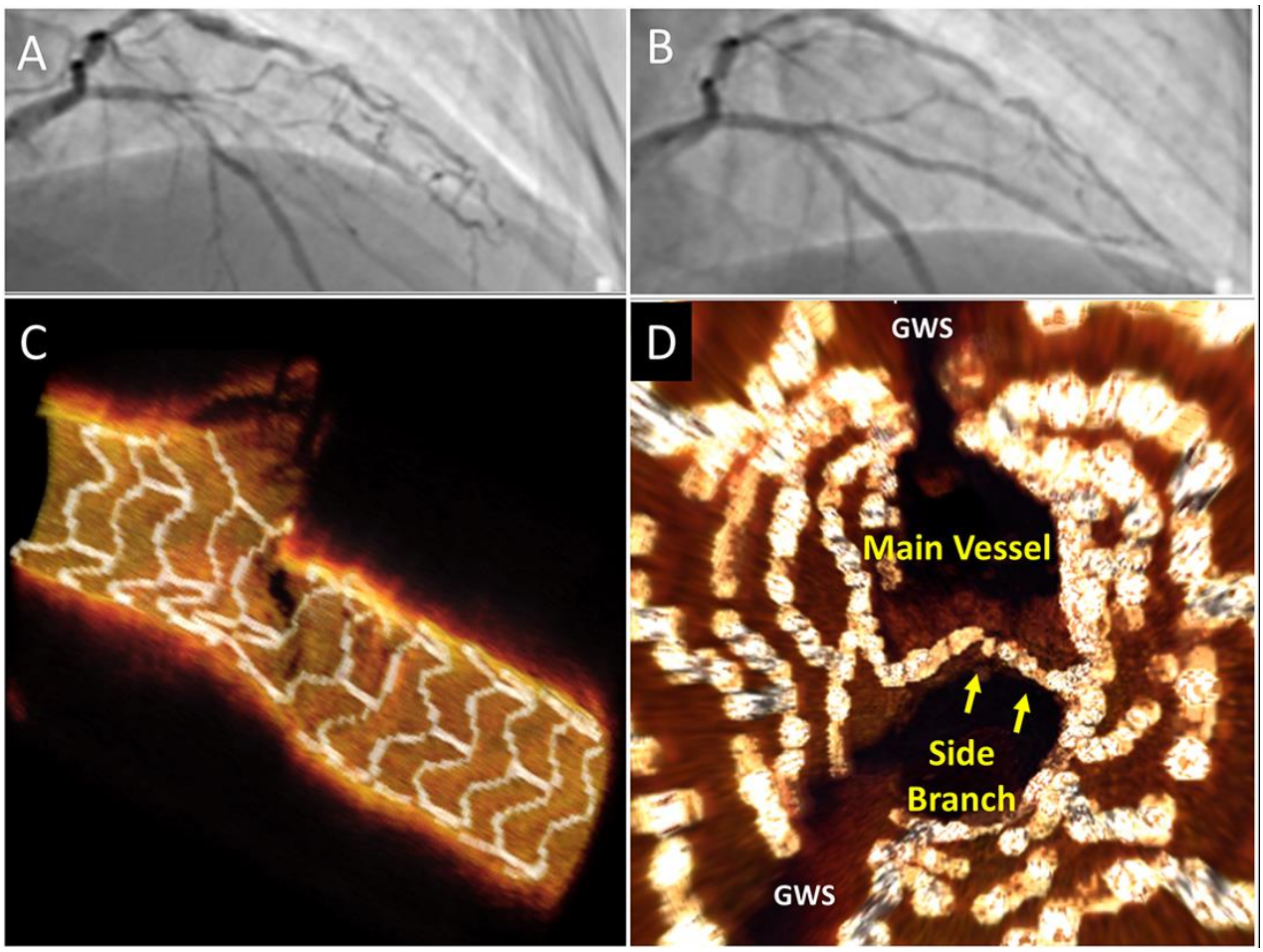

Supplementary Figure 3. Hybrid treatment of bifurcation lesion with BVS and metallic stent.

A left anterior descending artery/diagonal bifurcation lesion (A) was treated with an Absorb bioresorbable scaffold (main branch) and a metallic stent (side branch) (B). Final kissing balloon inflation was then performed at 4 atmospheres. 3D OCT reconstruction (C & D) was performed to ensure the preserved integrity of the BVS rings (yellow arrows) and complete opening of the side branch ostium.

Supplementary Figure 4.

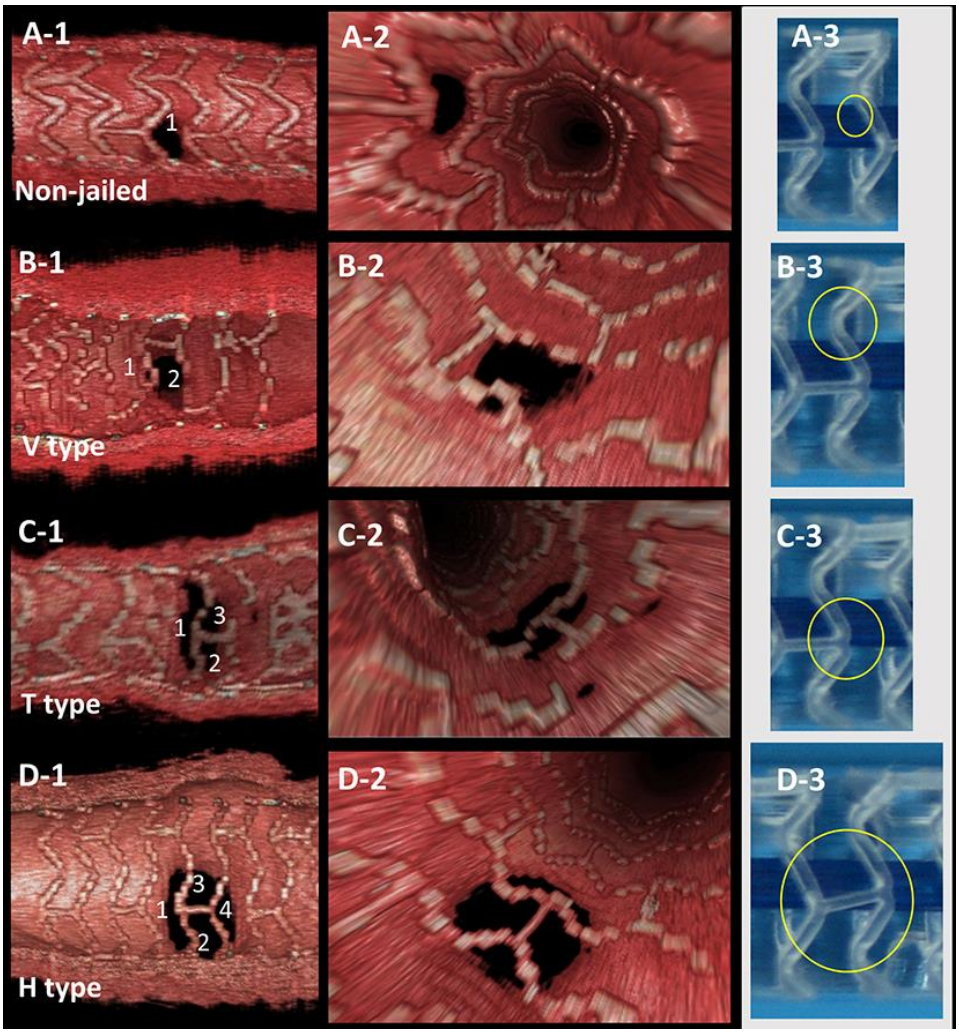

Supplementary Figure 4. The jailed side branch with the number of compartments created by the criss-cross of the struts as well as the configuration of the jailing struts.
The images in the first column (A-1, B-1, C-1 and D-1) show the classification of the jailed side branch ostium according to the number of compartments created by the overhanging struts with different configurations (i.e., V, T and H type). The images in the second column are fly-through images for each classification. The images in the third column show the configuration of the jailing struts.

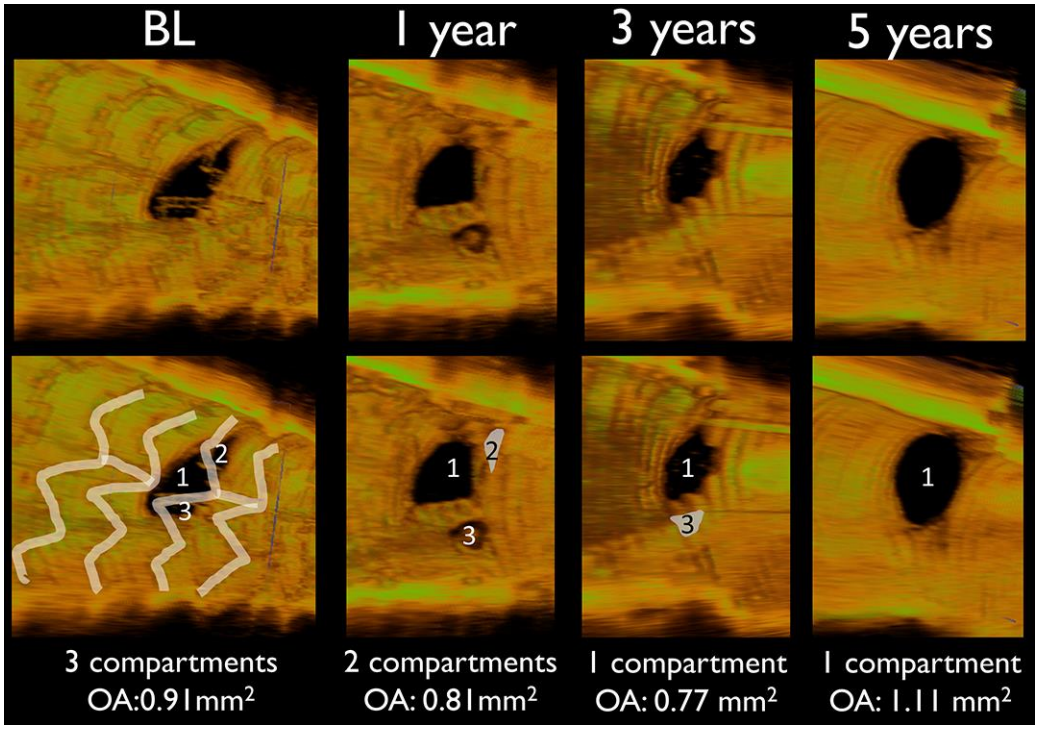

Supplementary Figure 5. Serial assessment of jailed side branch over five years.

Serial OCT images of the small side branch jailed by the bioresorbable scaffold struts. At baseline, polymeric struts formed three compartments with the side branch ostium. As the neointima grew, compartment #2 was covered at one year and compartment #3 was covered at three years, resulting in the reduction of the ostium area. At five years, the struts were no longer visible on OCT and the remaining compartment #1 enlarged.

OA: ostial area

Supplementary Table 1. Published clinical studies on OCT-guided PCI in bifurcation.

Author	Publication year	Study design	Device	Comparison	Endpoint	Results	References
Alegría-Barrero et al	2012	Retrospective single-centre study	XIENCE, BioMatrix, PROMUS Element, Resolute, CYPHER, TAXUS	OCT guidance (n=12) vs. angiography guidance (n=40)	% of malapposed struts	OCT guidance had a significantly lower number of malapposed stent struts (7.5%) compared to angiography guidance (15.8%, p=0.0009)	47
Viceconte et al	2013	Retrospective single-centre study	TAXUS, CoStar, CYPHER, Endeavor, Resolute, XIENCE, Endeavor	One-stent (n=30 bifurcations) vs. two-stent technique (n=15 bifurcations)	% of malapposed struts	Lesions treated with stenting of both MV and SB had a higher total rate of malapposition than those treated with stenting of the MV only (17.6% vs. 9.5%; p=0.0014). In MV only group, lesions treated with FD OCT-guided stent implantation (n=13) presented a lower rate of malapposition than those treated with conventional angiography-guided stent implantation (n=17) (7.1% vs. 17.5%; p=0.005).	103
Okamura et al	2014	Retrospective single-centre study	Endeavor, Nobori, PROMUS Element, XIENCE	Single arm (OCT guidance) (n=22 bifurcations)	% of incomplete stent apposition	The recrossing position was clearly visualised in 18/22 (81.8%) cases. In 13 cases, serial 3D OCT could be assessed both before and after final kissing balloon post-dilation (FKBD). %ISA of free carina type (n=7) at the bifurcation segment after FKBD was significantly smaller than that of the connecting to carina type (n=6) (0.7±0.9% vs. 12.2±6.5%, p=0.0074).	45
Dato et al	2017	Retrospective single-centre study	DES	Conservative (n=58 patients) and revascularised group (n=64 patients) according to the FD OCT LM criteria	TVF-free survival	TVF-free rate survival was not different between patients undergoing conservative management vs. revascularisation (HR 0.40, 95% CI: 0.10–1.61, p=0.20).	104
Nakamura et al	2017	Retrospective single-centre study	EES	Single arm (OCT guidance) (n=44 patients)	Minimum expansion index (MEI) by novel volumetric metrics and minimum stent area	The frequency of the underexpansion (<80%) was significantly greater in MEI compared with MSA [21 (47.7%) and 11 (25.0%), p=0.045].	51

Author	Publication year	Study design	Device	Comparison	Endpoint	Results	References
					(MSA) as conventional method		

Supplementary Table 2. Randomised controlled trials of OCT versus angiography-guided or IVUS-guided drug-eluting stent implantation with or without bifurcation lesions. Adapted from Mintz et al[105].

	Number of patients	Bifurcation	Endpoint	OCT	Angiography	IVUS	*p*-value (OCT vs. angiography)	*p*-value (OCT vs. IVUS)
ILUMIEN-III: OPTIMIZE-PCI trial[5]	450 (OCT:158, angiography:146, IVUS:146)	NA (planned two-stent bifurcations excluded)	OCT after PCI minimum stent area (non-inferiority vs. IVUS)	5·79 mm² (4·54–7·34)	5·49 mm² (4·39–6·59)	5·89 mm² (4·67–7·80)	0·12	0·001 non-inferiority; 0·42 for superiority
Habara et al[106]*	70 (OCT:35, IVUS:35)	NA (exclusion criteria)	IVUS stent expansion after PCI	6·1 mm² (2·2) (64·7% [13·7])		7·2 mm² (2·5) (80·3% [13·4])		0·04 (0·002)
DOCTORS trial[107]	240 (OCT:120, angiography:120)	NA	FFR after PCI	0·94 mm² (0·04)	0·92 mm² (0·05)			0·005
OPINION trial[4]	829 (OCT:414, IVUS:415)	OCT: 154/412 (37.4%) IVUS: 157/405 (38.8%)	12-month TVF† (non-inferiority vs. IVUS)	Frequency of TVF of 5·2%		4.90%		0·042 non-inferiority (log-rank 0·83)
DOCTOR Recross (ongoing)[108]	60 (angiography: 30, OCT: 30)	Dedicated for bifurcation	Cross-sectional stent strut malapposition in the main vessel bifurcation segment facing the side branch ostium after procedure	NA	NA	NA		

OPTIMUM (ongoing)[109]	103 (angiography-guided: 53, OCT-guided: 53)	Dedicated for bifurcation	Acute incomplete strut malapposition in bifurcation	NA	NA	NA
OCTOBER (ongoing)[110]	1,200 (angiography-guided: 600, OCT-guided: 600)	Dedicated for bifurcation	To compare median two-year clinical outcome after OCT-guided vs. standard guided revascularisation of patients requiring complex bifurcation stent implantation	NA	NA	NA

Data are median (IQR) and mean (SD) unless otherwise indicated.
*The frequency of TVF is indicated by the frequency (SD) in parentheses in the OCT and IVUS columns, and the p-value in parentheses in the comparison between the two techniques.
†TVF is a composite of cardiac death, target vessel-related myocardial infarction, and ischaemia-driven target vessel revascularisation.
FFR: fractional flow reserve; ISA: incomplete stent apposition; IVUS: intravascular ultrasound; NA: not available; OCT: optical coherence tomography; PCI: percutaneous coronary intervention; TVF: target vessel failure

Supplementary Table 3. Comparison of intravascular ultrasound versus optical coherence tomography in bifurcation treatment.

	IVUS	OCT
Pre-procedure		
Co-registration with angiogram	++	++
Sizing of vessel	++	+
Sizing of lumen	++	++
Assessment of plaque distribution	++	+
Plaque characterisation	++	+
Assessment of side branch ostium in the pullback of main branch	x	++
Determination of landing zone and stent length	++	++
During stent implantation		
Guidance of position of the guidewire towards the side branch	x	++
Post-procedure		
Evaluation of stent dimensions according to flow conservation law	++	++
Stent underexpansion	++	++
Edge dissection	+	++
ISA	+	++
Anatomic subgroups		
LMT lesion	++	+*

*except for ostial lesions. x: not usable; +: available; ++: helpful; ISA: incomplete stent apposition; IVUS: intravascular ultrasound; LMT: left main trunk; OCT: optical coherence tomography

Supplementary Table 4. OCT acquisition in bifurcations: tips and tricks.
Adapted from Holm et al[9]

Main vessel pullback
Evaluate if side branch ostium is visible after pullback. In case of conflicting wire shadow, consider manipulating wires and repeating pullback
Side branch pullback
Consider risk of side branch dissection before wiring
Avoid advancing an OCT catheter into a jailed side branch before opening of strut cells at side branch ostium
Ensure that side branch pullback extends into the main vessel
Left main coronary artery pullback
Aorto-ostial evaluation is not possible
Select maximum scan range to show widest possible image
Consider increased flow of flushing agent
Consider large guiding catheter for improved vessel clearing

Supplementary Table 5. Clinical studies with qualitative or quantitative endpoint using 3D OCT.

Author	Publication year	Study design	Enrolled patients	Device	Qualitative or quantitative analysis in 3D	Results of 3D OCT analysis
Alegría-Barrero et al[47]	2012	Single-centre study	52	XIENCE, BioMatrix, PROMUS Element, Resolute, CYPHER, TAXUS	Qualitative	2 case examples of distal rewiring and proximal rewiring
Fujino et al[70]	2013	Single-centre study	33	SES, EES	Qualitative	Presentation of a case with uncovered and malapposed struts
Grundeken et al[111]	2013	Single-centre study	12	Tryton	Qualitative	Presentation of a case with 100% strut coverage and an open ostium.
Grundeken et al[78]	2014	Single-centre study	10	Tryton	Qualitative	2 separate compartments in SB ostia: 2 patients, single compartment: 4 patients.
Okamura et al[45]	2014	Single-centre study	22	Endeavor, Nobori, PROMUS, XIENCE	Qualitative	Recrossing at the most distal cell: 10/13 (76.9%)
Yang et al[53]	2015	Single-centre study	41	SES, BES, EES	Quantitative	MLA of jailed side branch ostium by 3D OCT: 2.67 at post-intervention, 2.35 at 3–6M, 2.44 mm^2 at 1–2Y post-intervention (p=0.098).
Karanasos et al[15]	2015	Single-centre study	31	DES, BRS	Quantitative	SB ostial area by 3D cut-plane analysis from MB pullback better correlated with conventional analysis from SB pullback (R=0.927) than conventional analysis from MB with conventional analysis in SB (R=0.870, p=0.256).

Author	Publication year	Study design	Enrolled patients	Device	Qualitative or quantitative analysis in 3D	Results of 3D OCT analysis
Grundeken et al[79]	2015	Single-centre study	10	Tryton+Absorb	Qualitative	Strut shape in SB ostium: V shape (2), T shape (1), double T shape (1), "T and V" shape (1), a “T and double V” shape (1), and an “H and double V” shape (1)
Nakao et al[112]	2016	Multicentre study	21	Nobori	Qualitative	No stent links bridging from a carina: 90.9 in the LM–LCx stenting vs. 45.0% in the LM–LAD stenting (p=0.02).
Cho et al[52]	2016	Single-centre study	109	DES	Quantitative	The 3D OCT-measured MLA of the jailed side branch ostium: 2.91 before intervention, 2.37 mm^2 after intervention (p<0.01). Eccentricity index: 1.40 before intervention, 1.71 after intervention (p<0.01).
Kume et al[113]	2017	Single-centre study	29	PROMUS, Nobori, XIENCE, Resolute, Endeavor	Quantitative	SB orifice obstruction by neointima in the link group: 26.8%, in the no-link group: 9.5% (p = 0.049) at 18M
Onuma et al[114]	2017	Multicentre study	29	Absorb	Quantitative	Ostial area free from struts: 0.75 at baseline, 0.68 at 6M or 1Y, 0.63 at 2 or 3Y, 0.89 mm^2 at 5Y
Fujino et al[46]	2017	Single-centre study	38	SES, EES	Quantitative	The narrowing of LCX ostial area at 9M: 29.16% in SES vs. 2.46% in EES (p=0.001).
Pyxaras et al[55]	2017	Single-centre study	10	Tryton+DES (EES, ZES)	Quantitative	FKBI increased SB ostial area (4.93 vs. 7.43 mm^2, p<0.001)
Kini et a[115]	2017	Single-centre study	30	PROMUS	Quantitative	Post-stenting SB ostial stenosis (>50% area reduction) was observed in 30% of patients.

Supplementary Table 6. Case reports of bifurcation-dedicated stents with OCT evaluation.

Author	Publication year	Investigated device	Results of OCT analysis
Magro et al[116]	2010	Tryton	Good apposition was confirmed.
Adriaenssens et al[117]	2012	XIENCE SBA	OCT documented good apposition of struts at the ostium of the SB and absence of free floating struts at the level of the carina.
Pyxaras et al[118]	2013	Tryton	3D visualisation of bifurcation carina.
Antoniadis et al[119]	2013	Axxess	In reconstructed model using OCT and angiogram, flow velocity was higher in the central flow divider region and lower at the lateral aspects of the bifurcation.
van Ditzhuijzen et al[120]	2014	Nile Pax	After dissection induced by guidewire, OCT image could distinguish true lumen.
Chan et al[121]	2014	Axxess and BioMatrix	The segment covered by Axxess peeled away from the overlapping BioMatrix.
Hiltrop et al[122]	2016	Axxess and BioMatrix	3D IV-OCT reconstructions illustrate distal flaring of the Axxess device providing optimal SB coverage.

Supplementary Table 7. Clinical studies of bifurcation-dedicated stents with OCT evaluation.

Author	Year	Study design	Patients enrolled	Investigated device	Primary outcome	Secondary outcome	Results of OCT analysis
Tyczynski et al[82]	2009	Single-centre study	9	Tryton	Not specified	Not specified	Total % of malapposed struts per patient post procedure: 18.1%.
Verheye et al[83]	2009	Multicentre study	40	Stentys	Procedural success	Clinical, safety and angiographic parameters	Complete apposition of the stent struts post procedure (non-quantitative analysis by OCT)
Verheye et al[80]	2011	Multicentre study	60	Stentys BMS vs. Stentys DES	6M MACE	Complications, QCA, IVUS	OCT image in a case with good apposition at baseline, complete strut coverage and wide open ostium of the side branch at 6M.
Magro et al[81]	2011	Multicentre study	96	Tryton	Not specified	Not specified	A case example of OCT with good apposition post-procedure.
Grundeken et al[111]	2013	Single-centre study	12	Tryton	Not specified	Not specified	3D OCT at 1Y for case illustration purposes.
Dubois et al[86]	2013	Single-centre study	20	Tryton and XIENCE	Not specified	Not specified	Uncovered struts at 9M: 4.0, 0.7, 0, and 2.5% in the proximal MV, distal MV, SB, and polygon of confluence, respectively.
Grundeken et al[78]	2014	Single-centre study	10	Tryton and Absorb	Not specified	Not specified	Uncovered strut at 1Y: 0.7%. Incompletely apposed strut: 0.8%. Mean NIH thickness: 0.14±0.11 in the proximal MB, 0.19±0.11 in distal MB, and 0.34±0.19 mm in SB.
Ma et al[85]	2014	Multicentre study	28	Cappella Sideguard and balloon-expandable DES [EES, SES, PES, BES, and ZES]	Not specified	Not specified	Strut coverage at the bifurcation site at 6M: 100% in CS, 61% in DES.
Grundeken et al[79]	2015	Single-centre study	10	Tryton and Absorb	Not specified	Not specified	Incomplete apposition in the bifurcation area post-procedure: 26%.

Author	Year	Study design	Patients enrolled	Investigated device	Primary outcome	Secondary outcome	Results of OCT analysis
Dubois et al[84]	2016	Prospective multicentre RCT	40	Axxess+ BioMatrix vs. Culotte XIENCE	% of uncovered struts at 9M	Lumen and stent area, and neointimal thickness and area.	9M uncovered struts in the proximal MV (17.8% vs. 6.8%; p=0.19), bifurcation core (9.5% vs. 4.0%; p=0.17), distal MV (2.6% vs. 2.2%; p=0.09) and side branch (5.7% vs. 1.9%; p=0.14).
Pyxaras et al[55]	2017	Single-centre study	10	Tryton-SBS	Changes in FFR in the SB following FKBI	MB FFR; OCT metrics: minimum SB ostial diameter, maximum SB ostial diameter, SB ostial area; two-dimensional quantitative coronary angiography (2D QCA) metrics: reference vessel diameter (RVD), minimal lumen diameter (MLD) in proximal and distal MB and SB; three-dimensional (3D) QCA metrics: RVD, MLD in proximal and distal MB and SB.	Post-procedural change in SB ostial area: 4.93 vs. 7.43 mm^2, p<0.001, SB maximum diameter: 3.12 vs. 3.82 mm, p=0.003.

Supplementary Table 8. Ongoing device trials in bifurcation using OCT.

Name	Study design	Arms	Sample size	Purpose	Primary endpoint	Recruitment status	Reference
PCI With AXXESS Biolimus A9 Eluting Bifurcation Stent in Treating Coronary Artery Bifurcation Disease	Randomised	OCT-guided PCI vs. Angio-guided PCI and Axxess vs. BioMatrix Flex	Withdrawn before enrolment	1. To compare the safety and efficacy of AXXESS stent with conventional DES in patients with coronary artery bifurcation disease. 2. To assess the impact of optical coherence tomography (OCT) guidance on clinical outcomes following the stent type.	Late loss of side branch at 9 months after procedure	Withdrawn	123
COBRA II	Randomised	Axxess+Absorb vs. Modified T using Absorb	60	To compare healing responses on OCT after treatment of complex bifurcation lesions with Axxess+Absorb vs. Modified T using Absorb.	Changes in minimal luminal area at 30 months	Not yet recruiting	124
BIFSORB	Randomised	Absorb vs. DESolve	120	To compare the safety and vessel healing after treatment of simple bifurcation lesions with Absorb and DESolve BRS.	Clinical safety (myocardial infarction, revascularisation, death) at 6 months	Stopped due to discontinuation of Absorb sales	125
ORBID-FFR	Randomised	Lesion preparation using rotational atherectomy vs. cutting balloon angioplasty	150	To predict any changes in the side branch after stenting the main branch blood vessel using 3D OCT.	Side branch compromise at day 1	Recruiting	126
BIFSORB P-II	Observational	Bifurcation lesions treated with Magmaris BRS	20	To investigate the feasibility and safety and one-month healing pattern on OCT of the Magmaris BRS for treatment of coronary bifurcation lesions.	Combined endpoint of major procedural myocardial infarction, non-procedural myocardial infarction, target lesion failure and cardiac death at 1 month	Recruiting	127
OCTOBER (China)	Observational	Excel DES with a biodegradable polymer vs. CYPHER DES	100	To compare vessel healing at 6 months using OCT in Excel DES with a biodegradable polymer vs. CYPHER DES.	Neointimal stent strut coverage at 6 months	Unknown status	128

PEBCBLO	Observational	Paclitaxel-eluting PTCA-balloon dilation (SeQuent Please) in SB and drug-eluting stent (EXCEL stent) deployment in the main branch	30	To investigate the efficacy of Paclitaxel-eluting PTCA-balloon in SB and drug eluting stent (EXCEL stent) deployment in the main branch.	In-segment late lumen loss at 9 months	Unknown status	129

References

1. Thomas M, Hildick-Smith D, Louvard Y, Albiero R, Darremont O, Stankovic G, Pan M, Legrand V, Debruyne B, Lefèvre T. Percutaneous coronary intervention for bifurcation disease. A consensus view from the first meeting of the European Bifurcation Club. *EuroIntervention*. 2006;2:149-53.

2. Lassen JF, Holm NR, Stankovic G, Lefèvre T, Chieffo A, Hildick-Smith D, Pan M, Darremont O, Albiero R, Ferenc M, Louvard Y. Percutaneous coronary intervention for coronary bifurcation disease: consensus from the first 10 years of the European Bifurcation Club meetings. *EuroIntervention*. 2014;10:545-60.

3. Collet C, Onuma Y, Cavalcante R, Grundeken M, Généreux P, Popma J, Costa R, Stankovic G, Tu S, Reiber JHC, Aben JP, Lassen JF, Louvard Y, Lansky A, Serruys PW. Quantitative angiography methods for bifurcation lesions: a consensus statement update from the European Bifurcation Club. *EuroIntervention*. 2017;13:115-23.

4. Kubo T, Shinke T, Okamura T, Hibi K, Nakazawa G, Morino Y, Shite J, Fusazaki T, Otake H, Kozuma K, Ioji T, Kaneda H, Serikawa T, Kataoka T, Okada H, Akasaka T; OPINION Investigators. Optical frequency domain imaging vs. intravascular ultrasound in percutaneous coronary intervention (OPINION trial): one-year angiographic and clinical results. *Eur Heart J*. 2017;38:3139-47.

5. Ali ZA, Maehara A, Généreux P, Shlofmitz RA, Fabbiocchi F, Nazif TM, Guagliumi G, Meraj PM, Alfonso F, Samady H, Akasaka T, Carlson EB, Leesar MA, Matsumura M, Ozan MO, Mintz GS, Ben-Yehuda O, Stone GW; ILUMIEN III: OPTIMIZE PCI Investigators. Optical coherence tomography compared with intravascular ultrasound and with angiography to guide

coronary stent implantation (ILUMIEN III: OPTIMIZE PCI): a randomised controlled trial. *Lancet.* 2016;388:2618-28.

6. Lassen JF, Burzotta F, Banning AP, Lefevre T, Darremont O, Hildick-Smith D, Chieffo A, Pan M, Holm NR, Louvard Y, Stankovic G. Percutaneous coronary intervention for the left main stem and other bifurcation lesions: 12th consensus document from the European Bifurcation Club. *EuroIntervention*. 2018;13:1540-53.

7. Farooq V, Serruys PW, Heo JH, Gogas BD, Okamura T, Gomez-Lara J, Brugaletta S, Garcia-Garcia HM, van Geuns RJ. New insights into the coronary artery bifurcation hypothesis-generating concepts utilizing 3-dimensional optical frequency domain imaging. *JACC Cardiovasc Interv.* 2011;4:921-31.

8. Farooq V, Gogas BD, Okamura T, Heo JH, Magro M, Gomez-Lara J, Onuma Y, Radu MD, Brugaletta S, van Bochove G, van Geuns RJ, Garcia-Garcia HM, Serruys PW. Three-dimensional optical frequency domain imaging in conventional percutaneous coronary intervention: the potential for clinical application. *Eur Heart J.* 2013;34:875-85.

9. Holm NR, Adriaenssens T, Motreff P, Shinke T, Dijkstra J, Christiansen EH. OCT for bifurcation stenting: what have we learned? *EuroIntervention.* 2015;11 Suppl V:V64-70.

10. Shimamura K, Guagliumi G. Optical Coherence Tomography for Online Guidance of Complex Coronary Interventions. *Circ J.* 2016;80:2063-72.

11. Costa MA, Angiolillo DJ, Tannenbaum M, Driesman M, Chu A, Patterson J, Kuehl W, Battaglia J, Dabbons S, Shamoon F, Flieshman B, Niederman A, Bass TA; STLLR Investigators. Impact of stent deployment procedural factors on long-term effectiveness and safety of sirolimus-eluting stents (final results of the multicenter prospective STLLR trial). *Am J Cardiol.* 2008;101:1704-11.

12. Hebsgaard L, Nielsen TM, Tu S, Krusell LR, Maeng M, Veien KT, Raungaard B, Terkelsen CJ, Kaltoft A, Reiber JH, Lassen JF, Christiansen EH, Holm NR. Co-registration of optical coherence tomography and X-ray angiography in percutaneous coronary intervention. the Does Optical Coherence Tomography Optimize Revascularization (DOCTOR) fusion study. *Int J Cardiol.* 2015;182:272-8.

13. Kang SJ, Mintz GS, Kim WJ, Lee JY, Oh JH, Park DW, Lee SW, Kim YH, Lee CW, Park SW, Park SJ. Changes in left main bifurcation geometry after a single-stent crossover technique: an intravascular ultrasound study using direct imaging of both the left anterior descending and the left circumflex coronary arteries before and after intervention. *Circ Cardiovasc Interv.* 2011;4:355-61.

14. Miyazaki Y, Katagiri Y, Asano T, Collet C, Okamura T, Muramatsu T, Ozaki Y, van Geuns R, Onuma Y, Serruys P. Practical guide to using the Terumo OFDI system. OCT Atlas 2nd edition. 2017. https://www.pcronline.com/PCR-Publications/PCR-mobile-apps/OCT-Atlas-app

15. Karanasos A, Tu S, van Ditzhuijzen NS, Ligthart JM, Witberg K, Van Mieghem N, van Geuns RJ, de Jaegere P, Zijlstra F, Reiber JH, Regar E. A novel method to assess coronary artery bifurcations by OCT: cut-plane analysis for side-branch ostial assessment from a main-vessel pullback. *Eur Heart J Cardiovasc Imaging.* 2015;16:177-89.

16. Gould KL, Kirkeeide R, Johnson NP. Coronary branch steal: experimental validation and clinical implications of interacting stenosis in branching coronary arteries. *Circ Cardiovasc Imaging.* 2010;3:701-9.

17. Koo BK, Yang HM, Doh JH, Choe H, Lee SY, Yoon CH, Cho YK, Nam CW, Hur SH, Lim HS, Yoon MH, Park KW, Na SH, Youn TJ, Chung WY, Ma S, Park SK, Kim HS, Tahk SJ. Optimal intravascular ultrasound criteria and their accuracy for defining the functional

significance of intermediate coronary stenoses of different locations. *JACC Cardiovasc Interv.* 2011;4:803-11.

18. Han JK, Koo BK, Park KW, Ben-Dor I, Waksman R, Pichard A, Nam CW, Doh JH, Murata N, Tanaka N, Lee CH, Gonzalo N, Escaned J, Costa MA, Kubo T, Akasaka T, Hu X, Wang J, Yang HM, Yoon MH, Tahk SJ, Ma S, Park SK, Kim HS. Optimal intravascular ultrasound criteria for defining the functional significance of intermediate coronary stenosis: an international multicenter study. *Cardiology.* 2014;127:256-62.

19. Gonzalo N, Escaned J, Alfonso F, Nolte C, Rodriguez V, Jimenez-Quevedo P, Banuelos C, Fernandez-Ortiz A, Garcia E, Hernandez-Antolin R, Macaya C. Morphometric assessment of coronary stenosis relevance with optical coherence tomography: a comparison with fractional flow reserve and intravascular ultrasound. *J Am Coll Cardiol.* 2012;59:1080-9.

20. van der Giessen AG, Wentzel JJ, Meijboom WB, Mollet NR, van der Steen AF, van de Vosse FN, de Feyter PJ, Gijsen FJ. Plaque and shear stress distribution in human coronary bifurcations: a multislice computed tomography study. *EuroIntervention.* 2009;4:654-61.

21. Jia H, Hu S, Uemura S, Park SJ, Jang Y, Prasad A, Lee S, Soeda T, Abtahian F, Vergallo R, Tian J, Lee H, Stone PH, Yu B, Jang IK. Insights into the spatial distribution of lipid-rich plaques in relation to coronary artery bifurcations: an in-vivo optical coherence tomography study. *Coron Artery Dis.* 2015;26:133-41.

22. Gonzalo N, Garcia-Garcia HM, Regar E, Barlis P, Wentzel J, Onuma Y, Ligthart J, Serruys PW. In vivo assessment of high-risk coronary plaques at bifurcations with combined intravascular ultrasound and optical coherence tomography. *JACC Cardiovasc Imaging.* 2009;2:473-82.

23. Oviedo C, Maehara A, Mintz GS, Araki H, Choi SY, Tsujita K, Kubo T, Doi H, Templin B, Lansky AJ, Dangas G, Leon MB, Mehran R, Tahk SJ, Stone GW, Ochiai M, Moses JW. Intravascular ultrasound classification of plaque distribution in left main coronary artery bifurcations: where is the plaque really located? *Circ Cardiovasc Interv.* 2010;3:105-12.

24. Yakushiji T, Maehara A, Mintz GS, Saito S, Araki H, Oviedo C, Choi SY, Tahk SJ, Leon MB, Stone GW, Moses JW, Ochiai M. An intravascular ultrasound comparison of left anterior descending artery/first diagonal branch versus distal left main coronary artery bifurcation lesions. *EuroIntervention.* 2013;8:1040-6.

25. Kobayashi Y, Okura H, Kume T, Yamada R, Kobayashi Y, Fukuhara K, Koyama T, Nezuo S, Neishi Y, Hayashida A, Kawamoto T, Yoshida K. Impact of target lesion coronary calcification on stent expansion. *Circ J.* 2014;78:2209-14.

26. Mintz GS. Intravascular imaging of coronary calcification and its clinical implications. *JACC Cardiovasc Imaging.* 2015;8:461-71.

27. Tian W, Lhermusier T, Minha S, Waksman R. Rational use of rotational atherectomy in calcified lesions in the drug-eluting stent era: Review of the evidence and current practice. *Cardiovasc Revasc Med.* 2015;16:78-83.

28. Lindsay AC, Paulo M, Kadriye K, Tejeiro R, Alegria-Barrero E, Chan PH, Foin N, Syrseloudis D, Di Mario C. Predictors of stent strut malapposition in calcified vessels using frequency-domain optical coherence tomography. *J Invasive Cardiol.* 2013;25:429-34.

29. Karimi Galougahi K, Shlofmitz RA, Ben-Yehuda O, Généreux P, Maehara A, Mintz GS, Stone GW, Moses JW, Ali ZA. Guiding Light: Insights Into Atherectomy by Optical Coherence Tomography. *JACC Cardiovasc Interv.* 2016;9:2362-3.

30. Maejima N, Hibi K, Saka K, Akiyama E, Konishi M, Endo M, Iwahashi N, Tsukahara K, Kosuge M, Ebina T, Umemura S, Kimura K. Relationship Between Thickness of Calcium on Optical Coherence Tomography and Crack Formation After Balloon Dilatation in Calcified Plaque Requiring Rotational Atherectomy. *Circ J.* 2016;80:1413-9.

31. Lee MS, Singh V, Nero TJ, Wilentz JR. Cutting balloon angioplasty. *J Invasive Cardiol.* 2002;14:552-6.

32. de Ribamar Costa J Jr, Mintz GS, Carlier SG, Mehran R, Teirstein P, Sano K, Liu X, Lui J, Na Y, Castellanos C, Biro S, Dani L, Rinker J, Moussa I, Dangas G, Lansky AJ, Kreps EM, Collins M, Stone GW, Moses JW, Leon MB. Nonrandomized comparison of coronary stenting under intravascular ultrasound guidance of direct stenting without predilation versus conventional predilation with a semi-compliant balloon versus predilation with a new scoring balloon. *Am J Cardiol.* 2007;100:812-7.

33. Kawase Y, Saito N, Watanabe S, Bao B, Yamamoto E, Watanabe H, Higami H, Matsuo H, Ueno K, Kimura T. Utility of a scoring balloon for a severely calcified lesion: bench test and finite element analysis. *Cardiovasc Interv Ther.* 2014;29:134-9.

34. Bittl JA, Chew DP, Topol EJ, Kong DF, Califf RM. Meta-analysis of randomized trials of percutaneous transluminal coronary angioplasty versus atherectomy, cutting balloon atherotomy, or laser angioplasty. *J Am Coll Cardiol.* 2004;43:936-42.

35. Watanabe M, Uemura S, Kita Y, Sugawara Y, Goryo Y, Ueda T, Soeda T, Okayama S, Okura H, Kume T, Saito Y. Impact of branching angle on neointimal coverage of drug-eluting stents implanted in bifurcation lesions. *Coron Artery Dis.* 2016;27:682-9.

36. Watanabe M, Uemura S, Sugawara Y, Ueda T, Soeda T, Takeda Y, Kawata H, Kawakami R, Saito Y. Side branch complication after a single-stent crossover technique: prediction with frequency domain optical coherence tomography. *Coron Artery Dis.* 2014;25:321-9.

37. Gutierrez-Chico JL, Alegria-Barrero E, Teijeiro-Mestre R, Chan PH, Tsujioka H, de Silva R, Viceconte N, Lindsay A, Patterson T, Foin N, Akasaka T, di Mario C. Optical coherence tomography: from research to practice. *Eur Heart J Cardiovasc Imaging.* 2012;13:370-84.

38. Liu S, Sotomi Y, Eggermont J, Nakazawa G, Torii S, Ijichi T, Onuma Y, Serruys PW, Lelieveldt BPF, Dijkstra J. Tissue characterization with depth-resolved attenuation coefficient and backscatter term in intravascular optical coherence tomography images. *J Biomed Opt.* 2017;22:1-16.

39. Kubo T, Shinke T, Okamura T, Hibi K, Nakazawa G, Morino Y, Shite J, Fusazaki T, Otake H, Kozuma K, Akasaka T. Optical frequency domain imaging vs. intravascular ultrasound in percutaneous coronary intervention (OPINION trial): Study protocol for a randomized controlled trial. *J Cardiol.* 2016;68:455-60.

40. Otake H, Kubo T, Takahashi H, Shinke T, Okamura T, Hibi K, Nakazawa G, Morino Y, Shite J, Fusazaki T, Kozuma K, Ioji T, Kaneda H, Akasaka T; OPINION Investigators. Optical Frequency Domain Imaging Versus Intravascular Ultrasound in Percutaneous Coronary Intervention (OPINION Trial): Results From the OPINION Imaging Study. *JACC Cardiovasc Imaging*. 2018;11:111-23.

41. Ino Y, Kubo T, Matsuo Y, Yamaguchi T, Shiono Y, Shimamura K, Katayama Y, Nakamura T, Aoki H, Taruya A, Nishiguchi T, Satogami K, Yamano T, Kameyama T, Orii M, Ota S, Kuroi A, Kitabata H, Tanaka A, Hozumi T, Akasaka T. Optical Coherence Tomography Predictors for

Edge Restenosis After Everolimus-Eluting Stent Implantation. *Circ Cardiovasc Interv.* 2016 Oct;9(10).

42. Finet G, Gilard M, Perrenot B, Rioufol G, Motreff P, Gavit L, Prost R. Fractal geometry of arterial coronary bifurcations: a quantitative coronary angiography and intravascular ultrasound analysis. *EuroIntervention.* 2008;3:490-8.

43. Finet G, Derimay F, Motreff P, Guerin P, Pilet P, Ohayon J, Darremont O, Rioufol G. Comparative Analysis of Sequential Proximal Optimizing Technique Versus Kissing Balloon Inflation Technique in Provisional Bifurcation Stenting: Fractal Coronary Bifurcation Bench Test. *JACC Cardiovasc Interv.* 2015;8:1308-17.

44. Foin N, Torii R, Alegria E, Sen S, Petraco R, Nijjer S, Ghione M, Davies JE, Di Mario C. Location of side branch access critically affects results in bifurcation stenting: Insights from bench modeling and computational flow simulation. *Int J Cardiol.* 2013;168:3623-8.

45. Okamura T, Onuma Y, Yamada J, Iqbal J, Tateishi H, Nao T, Oda T, Maeda T, Nakamura T, Miura T, Yano M, Serruys PW. 3D optical coherence tomography: new insights into the process of optimal rewiring of side branches during bifurcational stenting. *EuroIntervention.* 2014;10:907-15.

46. Fujino Y, Attizzani GF, Tahara S, Naganuma T, Takagi K, Yabushita H, Wang W, Tanaka K, Matsumoto T, Kawamoto H, Yamada Y, Amano S, Watanabe Y, Warisawa T, Sato T, Mitomo S, Kurita N, Ishiguro H, Hozawa K, Tsukahara T, Motosuke M, Bezerra HG, Nakamura S, Nakamura S. Difference in vascular response between sirolimus-eluting- and everolimus-eluting stents in ostial left circumflex artery after unprotected left main as observed by optical coherence tomography. *Int J Cardiol.* 2017;230:284-92.

47. Alegria-Barrero E, Foin N, Chan PH, Syrseloudis D, Lindsay AC, Dimopolous K, Alonso-Gonzalez R, Viceconte N, De Silva R, Di Mario C. Optical coherence tomography for guidance of distal cell recrossing in bifurcation stenting: choosing the right cell matters. *EuroIntervention.* 2012;8:205-13.

48. Okamura T, Onuma Y, Garcia-Garcia HM, Bruining N, Serruys PW. High-speed intracoronary optical frequency domain imaging: implications for three-dimensional reconstruction and quantitative analysis. *EuroIntervention.* 2012;7:1216-26.

49. Okamura T, Nagoshi R, Fujimura T, Murasato Y, Yamawaki M, Ono S, Serikawa T, Hikichi Y, Norita H, Nakao F, Sakamoto T, Shinke T, Shite J. Impact of guidewire recrossing point into stent jailed side branch for optimal kissing balloon dilatation: core lab 3D optical coherence tomography analysis. *EuroIntervention*. 2018;13:e1785-93.

50. Burzotta F, Talarico GP, Trani C, De Maria GL, Pirozzolo G, Niccoli G, Leone AM, Saffioti S, Porto I, Crea F. Frequency-domain optical coherence tomography findings in patients with bifurcated lesions undergoing provisional stenting. *Eur Heart J Cardiovasc Imaging.* 2014;15:547-55.

51. Nakamura D, Attizzani GF, Nishino S, Tanaka K, Soud M, Pereira GT, Leygerman M, Fares A, Schnell A, Costa MA, Erglis A, Bezerra HG. New insight to estimate under-expansion after stent implantation on bifurcation lesions using optical coherence tomography. *Int J Cardiovasc Imaging.* 2017;33:1677-84.

52. Cho S, Kim JS, Ha J, Shin DH, Kim BK, Ko YG, Choi D, Jang Y, Hong MK. Three-Dimensional Optical Coherence Tomographic Analysis of Eccentric Morphology of the Jailed Side-Branch Ostium in Coronary Bifurcation Lesions. *Can J Cardiol.* 2016;32:234-9.

53. Yang PS, Ha J, Kim JS, Park S, Bae J, Shin DH, Kim BK, Ko YG, Choi D, Jang Y, Hong MK. Eccentric morphology of jailed side-branch ostium after stent crossover in coronary bifurcation lesions: a three-dimensional optical coherence tomographic analysis. *J Cardiol.* 2015;65:305-10.

54. Okamura T, Onuma Y, Garcia-Garcia HM, Regar E, Wykrzykowska JJ, Koolen J, Thuesen L, Windecker S, Whitbourn R, McClean DR, Ormiston JA, Serruys PW; ABSORB Cohort B Investigators. 3-Dimensional optical coherence tomography assessment of jailed side branches by bioresorbable vascular scaffolds: a proposal for classification. *JACC Cardiovasc Interv.* 2010;3:836-44.

55. Pyxaras SA, Toth GG, Di Gioia G, Ughi GJ, Tu S, Rusinaru D, Adriaenssens T, Reiber JHC, Leon MB, Bax JJ, Wijns W. Anatomical and functional assessment of Tryton bifurcation stent before and after final kissing balloon dilatation: Evaluations by three-dimensional coronary angiography, optical coherence tomography imaging and fractional flow reserve. *Catheter Cardiovasc Interv.* 2017;90:E1-10.

56. Radu MD, Räber L, Heo J, Gogas BD, Jorgensen E, Kelbaek H, Muramatsu T, Farooq V, Helqvist S, Garcia-Garcia HM, Windecker S, Saunamäki K, Serruys PW. Natural history of optical coherence tomography-detected non-flow-limiting edge dissections following drug-eluting stent implantation. *EuroIntervention.* 2014;9:1085-94.

57. De Cock D, Bennett J, Ughi GJ, Dubois C, Sinnaeve P, Dhooge J, Desmet W, Belmans A, Adriaenssens T. Healing course of acute vessel wall injury after drug-eluting stent implantation assessed by optical coherence tomography. *Eur Heart J Cardiovasc Imaging*. 2014;15:800-9.

58. Bouki KP, Sakkali E, Toutouzas K, Vlad D, Barmperis D, Phychari S, Riga M, Apostolou T, Stefanadis C. Impact of coronary artery stent edge dissections on long-term clinical outcome in

patients with acute coronary syndrome: an optical coherence tomography study. *Catheter Cardiovasc Interv.* 2015;86:237-46.

59. Chamié D, Bezerra HG, Attizzani GF, Yamamoto H, Kanaya T, Stefano GT, Fujino Y, Mehanna E, Wang W, Abdul-Aziz A, Dias M, Simon DI, Costa MA. Incidence, predictors, morphological characteristics, and clinical outcomes of stent edge dissections detected by optical coherence tomography. *JACC Cardiovasc Interv.* 2013;6:800-13.

60. Prati F, Romagnoli E, Burzotta F, Limbruno U, Gatto L, La Manna A, Versaci F, Marco V, Di Vito L, Imola F, Paoletti G, Trani C, Tamburino C, Tavazzi L, Mintz GS. Clinical Impact of OCT Findings During PCI: The CLI-OPCI II Study. *JACC Cardiovasc Imaging.* 2015;8:1297-305.

61. Kawamori H, Shite J, Shinke T, Otake H, Matsumoto D, Nakagawa M, Nagoshi R, Kozuki A, Hariki H, Inoue T, Osue T, Taniguchi Y, Nishio R, Hiranuma N, Hirata K. Natural consequence of post-intervention stent malapposition, thrombus, tissue prolapse, and dissection assessed by optical coherence tomography at mid-term follow-up. *Eur Heart J Cardiovasc Imaging.* 2013;14:865-75.

62. Taniwaki M, Radu MD, Zaugg S, Amabile N, Garcia-Garcia HM, Yamaji K, Jorgensen E, Kelbaek H, Pilgrim T, Caussin C, Zanchin T, Veugeois A, Abildgaard U, Juni P, Cook S, Koskinas KC, Windecker S, Räber L. Mechanisms of Very Late Drug-Eluting Stent Thrombosis Assessed by Optical Coherence Tomography. *Circulation*. 2016;133:650-60.

63. Sotomi Y, Onuma Y, Dijkstra J, Miyazaki Y, Kozuma K, Tanabe K, Popma JJ, de Winter RJ, Serruys PW, Kimura T. Fate of post-procedural malapposition of everolimus-eluting polymeric bioresorbable scaffold and everolimus-eluting cobalt chromium metallic stent in human coronary

arteries: sequential assessment with optical coherence tomography in ABSORB Japan trial. *Eur Heart J Cardiovasc Imaging.* 2018;19:59-66.

64. Steinberg DH, Mintz GS, Mandinov L, Yu A, Ellis SG, Grube E, Dawkins KD, Ormiston J, Turco MA, Stone GW, Weissman NJ. Long-term impact of routinely detected early and late incomplete stent apposition: an integrated intravascular ultrasound analysis of the TAXUS IV, V, and VI and TAXUS ATLAS workhorse, long lesion, and direct stent studies. *JACC Cardiovasc Interv.* 2010;3:486-94.

65. Guo N, Maehara A, Mintz GS, He Y, Xu K, Wu X, Lansky AJ, Witzenbichler B, Guagliumi G, Brodie B, Kellett MA Jr, Dressler O, Parise H, Mehran R, Stone GW. Incidence, mechanisms, predictors, and clinical impact of acute and late stent malapposition after primary intervention in patients with acute myocardial infarction: an intravascular ultrasound substudy of the Harmonizing Outcomes with Revascularization and Stents in Acute Myocardial Infarction (HORIZONS-AMI) trial. *Circulation*. 2010;122:1077-84.

66. Romagnoli E, Gatto L, La Manna A, Burzotta F, Taglieri N, Saia F, Amico F, Marco V, Ramazzotti V, Di Giorgio A, Di Vito L, Boi A, Contarini M, Castriota F, Mintz GS, Prati F. Role of residual acute stent malapposition in percutaneous coronary interventions. *Catheter Cardiovasc Interv.* 2017;90:566-75.

67. Authors/Task Force members, Windecker S, Kolh P, Alfonso F, Collet JP, Cremer J, Falk V, Filippatos G, Hamm C, Head SJ, Jüni P, Kappetein AP, Kastrati A, Knuuti J, Landmesser U, Laufer G, Neumann FJ, Richter DJ, Schauerte P, Sousa Uva M, Stefanini GG, Taggart DP, Torracca L, Valgimigli M, Wijns W, Witkowski A. 2014 ESC/EACTS Guidelines on myocardial revascularization: The Task Force on Myocardial Revascularization of the European Society of Cardiology (ESC) and the European Association for Cardio-Thoracic Surgery

(EACTS)Developed with the special contribution of the European Association of Percutaneous Cardiovascular Interventions (EAPCI). *Eur Heart J.* 2014;35:2541-619.

68. Muramatsu T, Garcia-Garcia HM, Onuma Y, Zhang YJ, Bourantas CV, Diletti R, Iqbal J, Radu MD, Ozaki Y, Serruys PW; TROFI investigators. Intimal flaps detected by optical frequency domain imaging in the proximal segments of native coronary arteries: an innocent bystander? Insights from the TROFI Trial. *Circ J.* 2013;77:2327-33.

69. Burzotta F, Dato I, Trani C, Pirozzolo G, De Maria GL, Porto I, Niccoli G, Leone AM, Schiavoni G, Crea F. Frequency domain optical coherence tomography to assess non-ostial left main coronary artery. *EuroIntervention*. 2015;10:e1-8.

70. Fujino Y, Attizzani GF, Bezerra HG, Wang W, Tahara S, Yamamoto H, Chamie D, Kanaya T, Mehanna E, Takagi K, Nakamura S, Costa MA. Serial assessment of vessel interactions after drug-eluting stent implantation in unprotected distal left main coronary artery disease using frequency-domain optical coherence tomography. *JACC Cardiovasc Interv.* 2013;6:1035-45.

71. Kang SJ, Ahn JM, Song H, Kim WJ, Lee JY, Park DW, Yun SC, Lee SW, Kim YH, Lee CW, Mintz GS, Park SW, Park SJ. Comprehensive intravascular ultrasound assessment of stent area and its impact on restenosis and adverse cardiac events in 403 patients with unprotected left main disease. *Circ Cardiovasc Interv*. 2011;4:562-9.

72. Tsuchida K, van der Giessen WJ, Patterson M, Tanimoto S, Garcia-Garcia HM, Regar E, Ligthart JM, Maugenest AM, Maatrijk G, Wentzel JJ, Serruys PW. In vivo validation of a novel three-dimensional quantitative coronary angiography system (CardiOp-B): comparison with a conventional two-dimensional system (CAAS II) and with special reference to optical coherence tomography. *EuroIntervention*. 2007;3:100-8.

73. Gonzalo N, Serruys PW, Garcia-Garcia HM, van Soest G, Okamura T, Ligthart J, Knaapen M, Verheye S, Bruining N, Regar E. Quantitative ex vivo and in vivo comparison of lumen dimensions measured by optical coherence tomography and intravascular ultrasound in human coronary arteries. [Article in English, Spanish]. *Rev Esp Cardiol.* 2009;62:615-24.

74. Okamura T, Onuma Y, Garcia-Garcia HM, van Geuns RJ, Wykrzykowska JJ, Schultz C, van der Giessen WJ, Ligthart J, Regar E, Serruys PW. First-in-man evaluation of intravascular optical frequency domain imaging (OFDI) of Terumo: a comparison with intravascular ultrasound and quantitative coronary angiography. *EuroIntervention*. 2011;6:1037-45.

75. Gutierrez-Chico JL, Serruys PW, Girasis C, Garg S, Onuma Y, Brugaletta S, Garcia-Garcia H, van Es GA, Regar E. Quantitative multi-modality imaging analysis of a fully bioresorbable stent: a head-to-head comparison between QCA, IVUS and OCT. *Int J Cardiovasc Imaging.* 2012;28:467-78.

76. Kubo T, Akasaka T, Shite J, Suzuki T, Uemura S, Yu B, Kozuma K, Kitabata H, Shinke T, Habara M, Saito Y, Hou J, Suzuki N, Zhang S. OCT compared with IVUS in a coronary lesion assessment: the OPUS-CLASS study. *JACC Cardiovasc Imaging*. 2013;6:1095-104.

77. Kobayashi Y, Kitahara H, Tanaka S, Okada K, Kimura T, Ikeno F, Yock PG, Fitzgerald PJ, Honda Y. Quantitative precision of optical frequency domain imaging: direct comparison with frequency domain optical coherence tomography and intravascular ultrasound. *Cardiovasc Interv Ther.* 2016;31:79-88.

78. Grundeken MJ, Garcia-Garcia HM, Kraak RP, Woudstra P, de Bruin DM, van Leeuwen TG, Koch KT, Tijssen JG, de Winter RJ, Wykrzykowska JJ. Side branch healing patterns of the Tryton dedicated bifurcation stent: a 1-year optical coherence tomography follow-up study. *Int J Cardiovasc Imaging.* 2014;30:1445-56.

79. Grundeken MJ, Hassell ME, Kraak RP, de Bruin DM, Koch KT, Henriques JP, van Leeuwen TG, Tijssen JG, Piek JJ, de Winter RJ, Wykrzykowska JJ. Treatment of coronary bifurcation lesions with the Absorb bioresorbable vascular scaffold in combination with the Tryton dedicated coronary bifurcation stent: evaluation using two- and three-dimensional optical coherence tomography. *EuroIntervention.* 2015;11:877-84.

80. Verheye S, Ramcharitar S, Grube E, Schofer JJ, Witzenbichler B, Kovac J, Hauptmann KE, Agostoni P, Wiemer M, Lefèvre T, Spaargaren R, Serruys PW, Garcia-Garcia HM, van Geuns RJ. Six-month clinical and angiographic results of the STENTYS® self-apposing stent in bifurcation lesions. *EuroIntervention*. 2011;7:580-7.

81. Magro M, Wykrzykowska J, Serruys PW, Simsek C, Nauta S, Lesiak M, Stanislawska K, Onuma Y, Regar E, van Domburg RT, Grajek S, Geuns RJ. Six-month clinical follow-up of the Tryton side branch stent for the treatment of bifurcation lesions: a two center registry analysis. *Catheter Cardiovasc Interv.* 2011;77:798-806.

82. Tyczynski P, Ferrante G, Kukreja N, Moreno-Ambroj C, Barlis P, Ramasami N, De Silva R, Beatt K, Di Mario C. Optical coherence tomography assessment of a new dedicated bifurcation stent. *EuroIntervention*. 2009;5:544-51.

83. Verheye S, Grube E, Ramcharitar S, Schofer JJ, Witzenbichler B, Kovac J, Hauptmann KE, Agostoni P, Wiemer M, Lefèvre T, Serruys PW, van Geuns RJ. First-in-man (FIM) study of the Stentys bifurcation stent--30 days results. *EuroIntervention*. 2009;4:566-71.

84. Dubois C, Bennett J, Dens J, De Cock D, Desmet W, Belmans A, Ughi GJ, Sinnaeve P, Vrolix M, D'hooge J, Adriaenssens T. COmplex coronary Bifurcation lesions: RAndomized comparison of a strategy using a dedicated self-expanding biolimus-eluting stent versus a culotte

strategy using everolimus-eluting stents: primary results of the COBRA trial. *EuroIntervention.* 2016;11:1457-67.

85. Ma S, Maehara A, Hauptmann KE, Guagliumi G, Valsecchi O, Vassileva AN, Appelman Y, Sangiorgi G, Prati F, Mintz GS. Mechanism of luminal patency of the self-expanding Sideguard sidebranch stent: evaluation by intravascular ultrasound and optical coherence tomography. *Catheter Cardiovasc Interv.* 2014;84:734-41.

86. Dubois C, Adriaenssens T, Ughi G, Wiyono S, Bennett J, Coosemans M, Ferdinande B, Sinnaeve P, D'Hooge J, Desmet W. Healing responses after bifurcation stenting with the dedicated TRYTON Side-Branch Stent™ in combination with XIENCE-V™ stents: a clinical, angiography, fractional flow reserve, and optical coherence tomography study: the PYTON (Prospective evaluation of the TRYTON Side-Branch Stent™ with an additional XIENCE-v™ everolimus-eluting stent in coronary bifurcation lesions) study. *Catheter Cardiovasc Interv.* 2013;81:E155-64.

87. Ferrante G, Kaplan AV, Di Mario C. Assessment with optical coherence tomography of a new strategy for bifurcational lesion treatment: the Tryton Side-Branch Stent. *Catheter Cardiovasc Interv.* 2009;73:69-72.

88. Nakazawa G, Otsuka F, Nakano M, Vorpahl M, Yazdani SK, Ladich E, Kolodgie FD, Finn AV, Virmani R. The pathology of neoatherosclerosis in human coronary implants bare-metal and drug-eluting stents. *J Am Coll Cardiol*. 2011;57:1314-22.

89. Räber L, Baumgartner S, Garcia HM, Kalesan B, Justiz J, Pilgrim T, Moschovitis A, Khattab AA, Buellesfeld L, Wenaweser P, Meier B, Serruys PW, Jüni P, Windecker S. Long-term vascular healing in response to sirolimus- and Paclitaxel-eluting stents: an optical coherence tomography study. *JACC Cardiovasc Interv.* 2012;5:946-57.

90. Farooq V, Vergouwe Y, Räber L, Vranckx P, Garcia-Garcia H, Diletti R, Kappetein AP, Morel MA, de Vries T, Swart M, Valgimigli M, Dawkins KD, Windecker S, Steyerberg EW, Serruys PW. Combined anatomical and clinical factors for the long-term risk stratification of patients undergoing percutaneous coronary intervention: the Logistic Clinical SYNTAX score. *Eur Heart J.* 2012;33:3098-104.

91. Tenekecioglu E, Poon EK, Collet C, Thondapu V, Torii R, Bourantas CV, Zeng Y, Onuma Y, Ooi AS, Serruys PW, Barlis P. The Nidus for Possible Thrombus Formation: Insight From the Microenvironment of Bioresorbable Vascular Scaffold. *JACC Cardiovasc Interv*. 2016;9:2167-8.

92. Ormiston JA, Webber B, Ubod B, Webster MW, White J. Absorb everolimus-eluting bioresorbable scaffolds in coronary bifurcations: a bench study of deployment, side branch dilatation and post-dilatation strategies. *EuroIntervention.* 2015;10:1169-77.

93. Ormiston J, Motreff P, Darremont O, Webber B, Guerin P, Webster M. Bioresorbable scaffolds on the bench. *EuroIntervention.* 2015;11 Suppl V:V166-9.

94. Tamburino C, Latib A, van Geuns RJ, Sabate M, Mehilli J, Gori T, Achenbach S, Alvarez MP, Nef H, Lesiak M, Di Mario C, Colombo A, Naber CK, Caramanno G, Capranzano P, Brugaletta S, Geraci S, Araszkiewicz A, Mattesini A, Pyxaras SA, Rzeszutko L, Depukat R, Diletti R, Boone E, Capodanno D, Dudek D. Contemporary practice and technical aspects in coronary intervention with bioresorbable scaffolds: a European perspective. *EuroIntervention*. 2015;11:45-52.

95. Latib A, Colombo A. Bifurcation disease: what do we know, what should we do? *JACC Cardiovasc Interv.* 2008;1:218-26.

96. Dzavik V, Colombo A. The absorb bioresorbable vascular scaffold in coronary bifurcations: insights from bench testing. *JACC Cardiovasc Interv.* 2014;7:81-8.

97. Di Mario C, Foin N, Colombo A. Kissing vanishing stents: are we trading ephemeral benefit for permanent damage? *EuroIntervention.* 2013;9:777-9.

98. Foin N, Mattesini A, Ghione M, Dall'ara G, Sen S, Nijjer S, Petraco R, Sgueglia GA, Davies JE, Di Mario C. Tools & techniques clinical: optimising stenting strategy in bifurcation lesions with insights from in vitro bifurcation models. *EuroIntervention.* 2013;9:885-7.

99. Fajadet J, Haude M, Joner M, Koolen J, Lee M, Tolg R, Waksman R. Magmaris preliminary recommendation upon commercial launch: a consensus from the expert panel on 14 April 2016. *EuroIntervention.* 2016;12:828-33.

100. Jaguszewski MJ, Cortes C, Gutiérrez-Chico JL. Implantation of magnesium-bioresorbable scaffolds in a bifurcation under optical coherence tomography guidance. *Eur Heart J.* 2017;38:2017-8.

101. Bennett J, Vanhaverbeke M, Vanden Driessche N, Hiltrop N, Adriaenssens T, Desmet W, Sinnaeve P, Dubois C. The drug-eluting absorbable magnesium vascular scaffold in complex coronary bifurcations: insights from an in-vivo multimodality imaging study. *EuroIntervention.* 2018;13:2036-46.

102. Tu S, Pyxaras SA, Li Y, Barbato E, Reiber JH, Wijns W. In vivo flow simulation at coronary bifurcation reconstructed by fusion of 3-dimensional X-ray angiography and optical coherence tomography. *Circ Cardiovasc Interv.* 2013;6:e15-7.

103. Viceconte N, Tyczynski P, Ferrante G, Foin N, Chan PH, Barrero EA, Di Mario C. Immediate results of bifurcational stenting assessed with optical coherence tomography. *Catheter Cardiovasc Interv.* 2013;81:519-28.

104. Dato I, Burzotta F, Trani C, Romano A, Paraggio L, Aurigemma C, Porto I, Leone AM, Niccoli G, Crea F. Optical coherence tomography guidance for the management of

angiographically intermediate left main bifurcation lesions: Early clinical experience. *Int J Cardiol.* 2017;248:108-13.

105. Mintz GS, Guagliumi G. Intravascular imaging in coronary artery disease. *Lancet.* 2017;390:793-809.

106. Habara M, Nasu K, Terashima M, Kaneda H, Yokota D, Ko E, Ito T, Kurita T, Tanaka N, Kimura M, Ito T, Kinoshita Y, Tsuchikane E, Asakura K, Asakura Y, Katoh O, Suzuki T. Impact of frequency-domain optical coherence tomography guidance for optimal coronary stent implantation in comparison with intravascular ultrasound guidance. *Circ Cardiovasc Interv.* 2012;5:193-201.

107. Meneveau N, Souteyrand G, Motreff P, Caussin C, Amabile N, Ohlmann P, Morel O, Lefrancois Y, Descotes-Genon V, Silvain J, Braik N, Chopard R, Chatot M, Ecarnot F, Tauzin H, Van Belle E, Belle L, Schiele F. Optical Coherence Tomography to Optimize Results of Percutaneous Coronary Intervention in Patients with Non-ST-Elevation Acute Coronary Syndrome: Results of the Multicenter, Randomized DOCTORS Study (Does Optical Coherence Tomography Optimize Results of Stenting). *Circulation.* 2016;134:906-17.

108. NCT02234804. The Does Optical Coherence Tomography Optimize Revascularization (DOCTOR) Recross Study (DOCTOR Recross). [Last accessed 19 Mar 2018]. Available at: https://clinicaltrials.gov/ct2/show/NCT02234804.

109. NCT02972489. On-line 3-dimensional Optical Frequency Domain Imaging to Optimize Bifurcation Stenting Using UltiMaster Stent: OPTIMUM Study. [Last accessed 19 Mar 2018]. Available at: https://clinicaltrials.gov/ct2/show/NCT02972489.

110. NCT03171311. The OCTOBER Trial - European Trial on Optical Coherence Tomography Optimized Bifurcation Event Reduction. [Last accessed 11 Oct 2017]. Available at: https://clinicaltrials.gov/ct2/show/NCT03171311.

111. Grundeken MJ, Agostoni P, Lesiak M, Koch KT, Voskuil M, de Winter RJ, Wykrzykowska JJ, Stella PR. Placement of Tryton Side Branch Stent only; a new treatment strategy for Medina 0,0,1 coronary bifurcation lesions. *Catheter Cardiovasc Interv.* 2013;82:E395-402.

112. Nakao F, Okamura T, Suetomi T, Yamada J, Nakamura T, Ueda T, Oda T, Kanemoto M, Ikeda Y, Fujii T, Yano M. Differences of side branch jailing between left main-left anterior descending artery stenting and left main-left circumflex artery stenting with Nobori biolimus-eluting stent. *Heart Vessels.* 2016;31:1895-903.

113. Kume T, Yamada R, Terumasa K, Tamada T, Imai K, Fukuhara K, Goryo Y, Kawamura A, Hiroshi O, Neishi Y, Uemura S. Neointimal coverage of jailed side branches in coronary bifurcation lesions: an optical coherence tomography analysis. *Coron Artery Dis.* 2018;29:114-8.

114. Onuma Y, Grundeken MJ, Nakatani S, Asano T, Sotomi Y, Foin N, Ng J, Okamura T, Wykrzykowska JJ, de Winter RJ, van Geuns RJ, Koolen J, Christiansen E, Whitbourn R, McClean D, Smits P, Windecker S, Ormiston JA, Serruys PW. Serial 5-Year Evaluation of Side Branches Jailed by Bioresorbable Vascular Scaffolds Using 3-Dimensional Optical Coherence Tomography: Insights From the ABSORB Cohort B Trial (A Clinical Evaluation of the Bioabsorbable Everolimus Eluting Coronary Stent System in the Treatment of Patients With De Novo Native Coronary Artery Lesions). *Circ Cardiovasc Interv.* 2017 Sep;10(9).

115. Kini AS, Vengrenyuk Y, Pena J, Yoshimura T, Panwar SR, Motoyama S, Kezbor S, Hasan CM, Palkhiwala S, Kovacic JC, Moreno P, Baber U, Mehran R, Narula J, Sharma SK. Plaque morphology predictors of side branch occlusion after provisional stenting in coronary bifurcation

lesion: Results of optical coherence tomography bifurcation study (ORBID). *Catheter Cardiovasc Interv.* 2017;89:259-68.

116. Magro M, van Geuns RJ. TheTryton side branch stent. *EuroIntervention*. 2010;6 Suppl J:J147-50.

117. Adriaenssens T, Ughi G, Coosemans M, Dubois C. Optical coherence tomography assessment of coverage of side branch ostium after implantation of Xience SBA dedicated coronary bifurcation system. *JACC Cardiovasc Interv.* 2012;5:1187-8.

118. Pyxaras SA, Tu S, Barbato E, Reiber JH, Wijns W. Optimization of Tryton dedicated coronary bifurcation system with coregistration of optical coherence tomography and fractional flow reserve. *JACC Cardiovasc Interv.* 2013;6:e39-40.

119. Antoniadis AP, Jaguszewski M, Maier W, Giannoglou GD, Luscher TF, Templin C. Geometrically correct three-dimensional optical coherence tomography: first self-expanding bifurcation stent evaluation. *Eur Heart J.* 2013;34:2715.

120. van Ditzhuijzen NS, Ligthart J, Tu S, van der Linden M, Regar E. Optical coherence tomography-guided bifurcation stenting of a coronary artery dissection. *Can J Cardiol.* 2014;30:956.e11-4.

121. Chan CY, Wu EB, Yan BP. Self-expanding stent peeling away from overlapping balloon-expandable stent causing late acquired aneurysm formation and stent malapposition. *JACC Cardiovasc Interv.* 2014;7:e35-7.

122. Hiltrop N, Ughi GJ, Dubois C, Adriaenssens T. Optical coherence tomography-based assessment of bifurcation stenting using the Axxess[a] Biolimus A9[a]-eluting stent system. *EuroIntervention.* 2016;11:1027.

123. NCT02384629. PCI With AXXESS Biolimus A9 Eluting Bifurcation Stent in Treating Coronary Artery Bifurcation Disease. [Last accessed 11 Oct 2017]. Available at: https://clinicaltrials.gov/ct2/show/NCT02384629.

124. NCT02628288. COmplex Bifurcation PCI: AXXESS Device + Absorb BVS, vs Modified T Stenting With Absorb BVS (COBRAII). [Last accessed 11 Oct 2017]. Available at: https://clinicaltrials.gov/ct2/show/NCT02628288.

125. NCT02973529. The Bioresorbable Implants for Scaffolding Obstructions in Randomized Bifurcations (BIFSORB) Study (BIFSORB). [Last accessed 11 Oct 2017]. Available at: https://clinicaltrials.gov/ct2/show/NCT02973529.

126. NCT03115580. Side Branch FFR After Provisional Stenting (ORBID-FFR). [Last accessed 11 Oct 2017]. Available at: https://clinicaltrials.gov/ct2/show/NCT03115580.

127. NCT03027856. The BIFSORB Pilot Study II (BIFSORB P-II). [Last accessed 11 Oct 2017]. Available at: https://clinicaltrials.gov/ct2/show/NCT03027856.

128. NCT01012583. Optical Coherence TomOgraphy Assessment of the Drug-Eluting Stent (OCTOBER). [Last accessed 11 Oct 2017]. Available at: https://clinicaltrials.gov/ct2/show/NCT01012583.

129. NCT02276846. Palpitate-Eluting Balloon Angioplasty in the Treatment of Coronary Bifurcation Lesion Evaluated by OCT (PEBCBLO). [Last accessed 11 Oct 2017]. Available at: https://clinicaltrials.gov/ct2/show/NCT02276846.